On stagnation points and streamline topology in vortex flows

By HASSAN AREF[1] AND MORTEN BRØNS[2]
1) *Department of Theoretical and Applied Mechanics, University of Illinois, Urbana, IL 61801 USA*
2) *Department of Mathematics, Technical University of Denmark, DK-2800 Lyngby, Denmark*

(Submitted to *J. Fluid Mech.*, Mon, Mar 3, 1997)

The problem of locating stagnation points in the flow produced by a system of N interacting point vortices in two dimensions is considered. The general solution, which follows from an 1864 theorem by Siebeck, that the stagnation points are the foci of a certain plane curve of class N–1 that has all lines connecting vortices pairwise as tangents, is stated and proved. This necessitates developing some of the mathematical apparatus of algebraic geometry. The case N=3, for which Siebeck's curve is a conic, is considered in some detail. In particular, it is shown that the classification of the type of conic coincides with the general classification of regimes of motion of the three vortices. A similarity result for the triangular coordinates of the stagnation point in a flow produced by three vortices with sum of strengths zero is found. The topologically distinct streamline patterns for the flow about three vortices are also determined, and partial results are given on the changes between these patterns as the motion evolves for two special sets of vortex strengths. The related problem of the location of stagnation points in a frame of reference moving with the vortices, when these are translating uniformly, is considered and an extension of Siebeck's theorem to this case is stated.

1. Introduction

It is well known that the equations of motion for inviscid fluid with vorticity in two dimensions admit various integrals arising from invariance of the equations of motion to translation and rotation of the coordinates. In particular, the linear impulse,

$$\mathbf{P} = \iint \zeta \mathbf{x}\, d\mathbf{x}, \tag{1.1}$$

where ζ is the component of vorticity perpendicular to the flow plane, is conserved (cf. Lamb, 1932). If the total vorticity of the flow is nonzero, this leads to the invariance of the *center of vorticity,* defined as the centroid of the vorticity distribution:

$$\mathbf{X} = \frac{\iint \zeta \mathbf{x}\, d\mathbf{x}}{\iint \zeta\, d\mathbf{x}}\,. \tag{1.2}$$

The invariance of this geometrically defined point might lead one to believe that a fluid particle placed at this position will remain stationary, or, in other words, that there is always a stagnation point of the flow at **X**. For certain simple cases, such as the motion of two identical vortices, this is, in fact, true, and follows from symmetry. However, in general **X** is not a stagnation point.

The simplest counter-example is provided by two point vortices of unequal circulation.

Let these be denoted Γ_1, Γ_2, and let their positions in the xy-plane be considered as points in a complex $z = x + iy$ plane. Then the equations of motion for the vortices are

$$\frac{d\bar{z}_1}{dt} = \frac{1}{2\pi i}\,\frac{\Gamma_2}{z_1 - z_2}\;; \qquad \frac{d\bar{z}_2}{dt} = \frac{1}{2\pi i}\,\frac{\Gamma_1}{z_2 - z_1} \tag{1.3}$$

(here and in the following overbars denote complex conjugation). It follows from (1.3), as a special case of (1.2), that the center of vorticity,

$$z_c = \frac{\Gamma_1 z_1 + \Gamma_2 z_2}{\Gamma_1 + \Gamma_2}\,, \tag{1.4}$$

remains constant in time. The fluid velocity (u,v) at the geometrically defined, invariant point z_c is given by the formula

$$u - iv = \frac{1}{2\pi i}\left(\frac{\Gamma_1}{z_c - z_1} + \frac{\Gamma_2}{z_c - z_2}\right) = \frac{(\Gamma_2 - \Gamma_1)(\Gamma_2 + \Gamma_1)^2}{2\pi i\,\Gamma_1\Gamma_2}\,\frac{1}{z_1 - z_2}, \tag{1.5}$$

from which we see that only in the special case $\Gamma_1 = \Gamma_2$ will both u and v vanish at z_c.

There is, of course, a stagnation point, z_s, in the flow also for $\Gamma_1 \neq \Gamma_2$ (unless $\Gamma_1 = -\Gamma_2$; see (1.7)). It is given by the equation

$$\frac{\Gamma_1}{z_s - z_1} + \frac{\Gamma_2}{z_s - z_2} = 0, \tag{1.6}$$

i.e., by

$$z_s = \frac{\Gamma_1 z_2 + \Gamma_2 z_1}{\Gamma_1 + \Gamma_2}\;; \tag{1.7}$$

(which should be read to imply that there is no finite stagnation point for $\Gamma_1 = -\Gamma_2$).

If we consider the geometrical midpoint of the line segment joining vortices 1 and 2,

$$z_m = \tfrac{1}{2}\,(z_1 + z_2), \tag{1.8}$$

we have that

$$z_m = \tfrac{1}{2}\,(z_s + z_c). \tag{1.9}$$

Hence, *the stagnation point and the center of vorticity are symmetrically placed with respect to the midpoint of the line joining the vortices.* It follows from this that the stagnation point moves in a circle about the center of vorticity, as do the two vortices.

Although the above example is quite elementary, it serves to sensitize us to the problem at hand. Perusal of the literature would suggest that general results about the location and motion of stagnation points in vortex flows are few and far between. On the other hand, stagnation points play an important role in the advection of a passive scalar by a vortex flow, and in the case of distributed vortices even for the dynamical evolution of the flow

itself. Any information that we can obtain about their number, location and motion thus seems very worthwhile.

This paper studies one of the simplest cases – the flow due to an assembly of point vortices of arbitrary strengths. Even in this case a considerable amount of work must be done before results of any generality emerge, and we must leave many questions incompletely answered or largely unexplored. For point vortices the problem of locating stagnation points is one of finding the roots of a certain polynomial. In practical terms finding such roots at an instant in time is not a particularly difficult problem, but the issue here is to derive general results, valid as the motion unfolds, as a function of the vortex strengths. We state the problem in §2, and deduce a first, simple result. The main body of the paper explains and explores a rather sophisticated geometrical characterization of the stagnation points as the foci of a certain curve. The results arise from the geometrical theorems of Julius Plücker and his followers, notably an 1864 theorem by Siebeck. This work does not seem to be known to the fluid mechanics community. Because of the use of less familiar mathematical concepts, such as the complex projective plane, we devote §3 to a brief 'tutorial' on background material that is needed for a statement and an appreciation of Siebeck's theorem. In §4 we then return to the vortex dynamics problem and explore the case of flow due to three vortices on the unbounded plane in some detail. This leads naturally in §5 to the problem of classification of the topology of streamlines in the flow about the three vortices, and a discussion of the dynamical conditions under which this streamline topology changes. We believe to have found all possible streamline topologies for three vortices, and we state some results on the bifurcations of streamline patterns using the known solutions for three-vortex motion. However, a complete solution of the bifurcation problem appears quite involved, and is not accomplished in this paper. In the case of three vortices of zero total strength a curious similarity law for the location of the single stagnation point is found, and this result determines the streamline patterns and their evolution in this case. In §6 we extend the treatment to the problem of the streamline pattern following a system of translating vortices in fixed, relative positions. Again, we explore the case of three vortices in some detail. This generalizes the notion of the 'atmosphere' of a vortex pair first considered by Kelvin and later, for vortices of arbitrary relative strength, by Morton (1932). Our final §7 contains some brief concluding remarks.

A preliminary account of this work was presented at the Forty-eighth Annual Meeting of the American Physical Society, Division of Fluid Dynamics, in Irvine, CA (Aref & Brøns 1995).

2. The general problem

Since the velocity (u,v) induced by a system of N point vortices is of the form

$$u - iv = \frac{1}{2\pi i} \sum_{\alpha=1}^{N} \frac{\Gamma_\alpha}{z - z_\alpha}, \tag{2.1}$$

it follows that the stagnation points are the roots of the polynomial

$$\begin{aligned} P(z) = {} & \Gamma_1(z - z_2)(z - z_3) \ldots (z - z_N) + \\ & \Gamma_2(z - z_1)(z - z_3) \ldots (z - z_N) + \ldots + \\ & \Gamma_N(z - z_1)(z - z_2) \ldots (z - z_{N-1}). \end{aligned} \tag{2.2}$$

Expanding this in powers of z, the leading terms are

$$P(z) = (\Gamma_1 + \Gamma_2 + \ldots + \Gamma_N)\, z^{N-1} - (\Gamma_1 z_2 + \Gamma_1 z_3 + \ldots + \Gamma_1 z_N + \Gamma_2 z_1 + \Gamma_2 z_3 + \ldots + \Gamma_2 z_N + \ldots + \Gamma_N z_1 + \Gamma_N z_2 + \ldots + \Gamma_N z_{N-1})\, z^{N-2} + \ldots \tag{2.3}$$

Thus, if the sum of the vortex strengths does not vanish, there are N–1 roots of the polynomial, i.e., N–1 stagnation points (although some of these may, of course, coincide). When the sum of the vortex strengths vanishes, there are at most N–2 distinct stagnation points.

The coefficient of z^{N-2} in (2.3) may be written as

$$-(\Gamma_1 + \Gamma_2 + \ldots + \Gamma_N) \sum_{\alpha=1}^{N} z_\alpha + \sum_{\alpha=1}^{N} \Gamma_\alpha z_\alpha = (\Gamma_1 + \Gamma_2 + \ldots + \Gamma_N)(z_c - N z_m), \tag{2.4}$$

where z_m denotes the 'midpoint' or centroid of the positions, defined as:

$$z_m = \frac{1}{N} \sum_{\alpha=1}^{N} z_\alpha, \tag{2.5}$$

and, when the sum of strengths is non-zero, the center of vorticity, z_c, is the discrete vortex counterpart of (1.2):

$$z_c = \frac{\sum_{\alpha=1}^{N} \Gamma_\alpha z_\alpha}{\sum_{\alpha=1}^{N} \Gamma_\alpha}. \tag{2.6}$$

The case when both the sum of strengths and the total impulse (which appears as the numerator of (2.6)) vanish is special: In this case the coefficient of z^{N-2} is zero, and there are at most N–3 different stagnation points. We remark that the four-vortex problem, which is in general non-integrable, is in fact integrable in this special case (Eckhardt & Aref 1988; Eckhardt 1988). There is then at most one stagnation point in the flow.

For the case of N vortices we may now write a generalization of Eq.(1.9). If we denote the stagnation points by $z_1^{(S)}$, ..., $z_{N-1}^{(S)}$, we have

$$P(z) = (\Gamma_1 + \Gamma_2 + \ldots + \Gamma_N)(z - z_1^{(S)}) \ldots (z - z_{N-1}^{(S)}). \tag{2.7}$$

Expanding and comparing coefficients to (2.3), we see that in general

$$N z_m - z_c = z_1^{(S)} + \ldots + z_{N-1}^{(S)} \tag{2.8}$$

which may be written

$$\sum_{n=1}^{N-1} (z_n^{(S)} - z_m) = z_m - z_c. \tag{2.9}$$

Thus, *the sum of the vectors from the midpoint to the stagnation points equals the vector from the center of vorticity to the midpoint.* In particular, for identical vortices the

midpoint and the center of vorticity coincide, and the sum of the vectors from the midpoint to the stagnation points vanishes. For N=2 Eq.(2.9) reduces to (1.9).

Returning to the polynomial P(z) – in the form (2.2) – we see that the problem of locating the stagnation points of a flow induced by N point vortices is equivalent to the problem of finding the location in the complex plane of the roots of this polynomial. The problem of locating the roots of a polynomial given through its coefficients has spawned a large literature in mathematics, much of which will be unfamiliar to the fluid mechanics community, and certainly was unfamiliar to us when we began this investigation. The monograph by Marden (1949) provides a useful starting point for pursuing this literature. We were pleasantly surprised to find that there exists a precise geometrical characterization of the location of the stagnation points for a system of N vortices as the foci of a certain explicitly given curve (of *class* N–1; we shall explain the notion of the class of a curve in §3(b)) in the plane. The main result goes back to a paper by F. H. Siebeck (1864). Siebeck's work is based on the geometry of Julius Plücker (1801-1868), and utilizes the complex projective plane. The result is re-stated and elaborated by several later authors. We found the account by Heawood (1906) to be one of the more useful. The present paper arose in large measure from our attempts to understand Siebeck's theorem and its potential utility in determining the stagnation points of a vortex flow.

Siebeck's theorem is one of the first results in Marden's book – it is stated and proved on pp.9-12 – and is, in fact, related there to the problem of finding the stagnation points of a system of sources and sinks! While we might simply refer the reader to Marden (1949), we feel it is appropriate to provide a quick 'tutorial' on the geometry of the complex projective plane in order to introduce various concepts and establish our notation, state and prove the theorem, and then proceed to a more detailed study of special cases. The three-vortex problem, in particular, where the curves that arise in Siebeck's theorem are conic sections, deserves further elaboration. Our main contribution, then, is a detailed discussion of the location of stagnation points in the three-vortex problem, and the attendant changes in topology that occur in the streamline pattern as the vortices (and stagnation points) move. There are, as we shall see, interesting connections to the general classification of three-vortex motion given several years ago (Synge 1949, Aref 1979). For the case of three vortices with sum of strengths equal to zero, where we have a very detailed understanding of the motion due to the work of Rott (1989) and Aref (1989), we are led to a scaling law for the single stagnation point, that would seem difficult to find without the formalism pursued here. In general we may say that the merit of Siebeck's theorem is the geometric characterization of the stagnation points as a function of the vortex positions and strengths that it provides. In terms of actual calculation, the extraction of roots of a low order polynomial is a relatively trivial procedure, and efficient, direct, numerical methods for solving this problem can easily be given. We elaborate on this statement in §7.

3. The complex projective plane and Siebeck's theorem[1]

We consider the set of triples of complex numbers $(x_1,x_2,x_3) \neq (0,0,0)$. Two such triples, (x_1,x_2,x_3) and (y_1,y_2,y_3), are considered to be equivalent if there exists a complex number, c, such that $(x_1,x_2,x_3) = (cy_1,cy_2,cy_3)$. Due to this equivalence relation the set of

1) The mathematical apparatus developed here was treated by numerous authors in texts on algebraic geometry of the last century, e.g., Salmon (1854), Ferrers (1866). These treatments are, in principle, elementary, yet often appear rather inaccessible. Modern treatments, on the other hand, are often phrased in such general mathematical terms as to be difficult to use for purposes of practical calculation. An important exception is Ch. 12 of the book by Coxeter (1993), where much of the classical material is summarized using modern notation and point of view.

triples is divided into equivalence classes. The set of equivalence classes constitutes the *complex projective plane* $\mathbf{P}^2$. Computations in $\mathbf{P}^2$ are performed on representatives of the equivalence classes, so when we use terms such as "the point (x_1,x_2,x_3)", we mean the equivalence class that contains (x_1,x_2,x_3). The equivalence of proportional triples implies that the only algebraic expressions that are meaningful are homogeneous in the coordinates, and thus that during calculations dropping a common factor is permitted. We shall often designate a coordinate triple (x_1,x_2,x_3) by the symbol $(\mathbf{x})$.

For any point in $\mathbf{P}^2$ corresponding to a triple (x_1,x_2,x_3) with $x_3\neq 0$, there corresponds a unique "point" in the set of complex pairs $\mathbf{C}^2$, viz $(x_1/x_3,x_2/x_3)$. Thus, $\mathbf{P}^2$ contains $\mathbf{C}^2$, but also has additional elements, viz all those triples for which $x_3=0$. These points will be called *ideal elements* of $\mathbf{P}^2$ or *points at infinity.* The usual plane, $\mathbf{R}^2$, viewed either as the complex plane, $\mathbf{C}$, or as the set of real pairs, is contained within $\mathbf{C}^2$. In order to distinguish it from the projective plane, we shall refer to $\mathbf{R}^2$ as the *affine plane.* It will be useful to consider statements of analytical geometry in the affine plane, which is where our vortices and stagnation points ultimately reside, as statements about entities in $\mathbf{P}^2$; to perform various manipulations in $\mathbf{P}^2$; and then to interpret the results in the affine plane. We need next to familiarize ourselves with the geometry in $\mathbf{P}^2$, and to see how to translate results back and forth between $\mathbf{R}^2$ and $\mathbf{P}^2$.

a. *Lines*

In $\mathbf{R}^2$ a line is given by an expression of the form

$$ax + by + c = 0 \tag{3.1}$$

where x and y are the usual coordinates of a variable point and a, b, c are certain numbers determining the line in question. Setting $x = x_1/x_3$, $y = x_2/x_3$, and multiplying through by x_3, we obtain an equation of the form

$$u_1x_1 + u_2x_2 + u_3x_3 = 0 \tag{3.2}$$

as the equation for a line in $\mathbf{P}^2$ (where x_1, x_2 and x_3 now are allowed to be complex). Note that this expression is, indeed, homogeneous in the coordinates. The points on the line are those triples (x_1,x_2,x_3) (as representatives of equivalence classes, as discussed above) for which the equation is satisfied. It is, therefore, natural to think of the triple $[u_1,u_2,u_3]$ as characterizing the line, and we call this triple the *coordinates of the line.* When we need to make the distinction, we will refer to (x_1,x_2,x_3) as the point coordinates (and use round brackets), and to $[u_1,u_2,u_3]$ as the line coordinates (and use square brackets). Note that $[u_1,u_2,u_3]$ is again determined only up to a constant of proportionality. Just as we may read (3.2) as the equation of all the points (x_1,x_2,x_3) on the line $[u_1,u_2,u_3]$, we may also read it as the equation of all the lines $[u_1,u_2,u_3]$ passing through the point (x_1,x_2,x_3). In this way we begin to see the *duality* of points and lines in the formulation of geometry in the projective plane $\mathbf{P}^2$. All the ideal elements in $\mathbf{P}^2$ are on a line with coordinates [0,0,1], the *ideal line* or the *line at infinity.*

We shall often designate a triple of line coordinates $[u_1,u_2,u_3]$ simply by $[\mathbf{u}]$, and we shall use the convention of summing over repeated indices to write an equation such as (3.2) in the form

$$u_i x_i = 0. \tag{3.2'}$$

Two different lines in $\mathbf{P}^2$ always intersect. To find the point of intersection of $[u_1,u_2,u_3]$ and $[v_1,v_2,v_3]$ we must solve the system

$$u_1x_1 + u_2x_2 + u_3x_3 = 0, \tag{3.3a}$$
$$v_1x_1 + v_2x_2 + v_3x_3 = 0. \tag{3.3b}$$

It is easily seen that the solution, up to a common factor (which is unimportant), is

$$(x_1,x_2,x_3) = (u_2v_3 - u_3v_2,\ u_3v_1 - u_1v_3,\ u_1v_2 - u_2v_1), \tag{3.4}$$

and this is $\neq(0,0,0)$ unless $[u_1,u_2,u_3]$ and $[v_1,v_2,v_3]$ are proportional, i.e., so long as the lines are different. Two lines will intersect in an ideal point, i.e., $u_1v_2 - u_2v_1$ will vanish, precisely when the lines interpreted in $\mathbf{R}^2$ are parallel[2].

Similarly, we may show that there is just one line through two different points $(\mathbf{x}) = (x_1,x_2,x_3)$ and $(\mathbf{y}) = (y_1,y_2,y_3)$. For this line, $[\mathbf{u}] = [u_1,u_2,u_3]$, must satisfy

$$u_1x_1 + u_2x_2 + u_3x_3 = 0, \tag{3.5a}$$
$$u_1y_1 + u_2y_2 + u_3y_3 = 0. \tag{3.5b}$$

Hence

$$[u_1,u_2,u_3] = [x_2y_3 - x_3y_2,\ x_3y_1 - x_1y_3,\ x_1y_2 - x_2y_1], \tag{3.6}$$

and this is $\neq(0,0,0)$ unless $(\mathbf{x})$ and $(\mathbf{y})$ are proportional, i.e., unless they correspond to the same point in $\mathbf{P}^2$. We see the duality between a line through two points and a point at the intersection of two lines.

b. *General curves: order, class and tangents*

Let us consider a general algebraic curve $F(x_1,x_2,x_3) = 0$, where F is some homogeneous polynomial in its three variables. If F is of degree n, we say that the curve is of *order* n. A line in the projective plane will intersect a curve of order n in n points.

Using the homogeneity of F, viz $F(\lambda x_1,\lambda x_2,\lambda x_3) = 0$ for any λ, we differentiate with respect to λ and set $\lambda = 1$ to obtain:

$$\frac{\partial F}{\partial x_i}\, x_i = 0, \tag{3.7}$$

or, in "vector notation," $\mathbf{x} \cdot \nabla F = 0$.

On the other hand, the tangent to the curve at $(\mathbf{x})$ is the line connecting $(\mathbf{x})$ to an infinitesimally close point on the curve $(\mathbf{x} + d\mathbf{x})$. This line is $[\mathbf{u}] = [\mathbf{x} \times d\mathbf{x}]$. But $(\mathbf{x} + d\mathbf{x})$ is also on the curve, so $F(\mathbf{x} + d\mathbf{x}) = 0 = F(\mathbf{x}) + d\mathbf{x} \cdot \nabla F + \ldots$, or $d\mathbf{x} \cdot \nabla F = 0$. It follows from this and the preceding result, $\mathbf{x} \cdot \nabla F = 0$, that $[\mathbf{x} \times d\mathbf{x}] = [\nabla F]$ (recall that a constant

2) We may also use the notation of vectors in 3D, e.g., by thinking of the incidence relation (3.2) as a 'scalar product' $\mathbf{u}\cdot\mathbf{x} = 0$, and the intersection of two lines $[\mathbf{u}]$ and $[\mathbf{v}]$ as being the point $(\mathbf{u}\times\mathbf{v})$. We show in (3.6) that the line connecting $(\mathbf{x})$ and $(\mathbf{y})$ is $[\mathbf{x}\times\mathbf{y}]$.

of proportionality may be dropped). Thus, the line $[\mathbf{u}] = [\nabla F] = [\frac{\partial F}{\partial \mathbf{x}}]$ is the tangent to the curve at point $(\mathbf{x})$.

We may also consider an expression of the form $\Phi[u_1,u_2,u_3] = 0$, where Φ is some homogeneous polynomial in its three variables. The lines that satisfy this equation will in general have an envelope, which is a curve in the plane. If Φ is of degree m, we say that this curve is of *class* m. Through any point in the projective plane there will be m tangents to a curve of class m.

Again, by homogeneity

$$\frac{\partial \Phi}{\partial u_i}\, u_i = 0, \tag{3.8}$$

or $\mathbf{u} \bullet \nabla\Phi = 0$.

A point on the curve, $(\mathbf{x})$, arises by finding the intersection of two infinitesimally close tangents $[\mathbf{u}]$ and $[\mathbf{u} + d\mathbf{u}]$. The point of intersection of these two lines is $(\mathbf{x}) = (\mathbf{u} \times d\mathbf{u})$. But $\Phi[\mathbf{u} + d\mathbf{u}] = \Phi[\mathbf{u}] + d\mathbf{u} \bullet \nabla\Phi + \ldots = 0$, or $d\mathbf{u} \bullet \nabla\Phi = 0$. It follows from this and the preceding result, $\mathbf{u} \bullet \nabla\Phi = 0$, that $(\mathbf{u} \times d\mathbf{u}) = (\nabla\Phi)$ (a constant of proportionality may again be dropped). Thus, $(\mathbf{x}) = (\nabla\Phi) = (\frac{\partial \Phi}{\partial \mathbf{u}})$ is the point of tangency of the tangent $[\mathbf{u}]$.

The preceding considerations show us how to get the equation in line coordinates of a curve given in point coordinates and *vice versa.* Thus, to get the equation of the curve $\Phi[\mathbf{u}] = 0$ in point coordinates, write out the derivative, $\frac{\partial \Phi}{\partial \mathbf{u}}$, solve the three equations $\mathbf{x} = \frac{\partial \Phi}{\partial \mathbf{u}}$ for the u's in terms of the x's, and substitute the result into $\Phi[u_1,u_2,u_3] = 0$. Similarly, to get the equation of the curve $F(\mathbf{x}) = 0$ in line coordinates, write out the derivative, $\frac{\partial F}{\partial \mathbf{x}}$, solve the three equations $\mathbf{u} = \frac{\partial F}{\partial \mathbf{x}}$ for the x's in terms of the u's, and substitute the result into $F(x_1,x_2,x_3) = 0$.

c. *Conics*

A conic (or conic section) in $\mathbf{R}^2$ is given by a quadratic polynomial in the coordinates x and y. Again setting $x = x_1/x_3$, $y = x_2/x_3$, and multiplying through by x_3, we arrive at a homogeneous quadratic form in x_1, x_2, and x_3. We may write this *point conic* in $\mathbf{R}^2$ as

$$F(x_1,x_2,x_3) = a_{ij}x_i x_j = 0 \tag{3.9}$$

The conic is singular if the determinant of the symmetric coefficient matrix vanishes. It is in general *a curve of order 2.* In order to classify the conic we need to consider the sign of the determinant of the minor $\begin{bmatrix} a_{11} & a_{12} \\ a_{21} & a_{22} \end{bmatrix}$. The conic is an ellipse, parabola or hyperbola according as this determinant is positive, zero, or negative.

The tangent to the conic at $(\mathbf{x})$ is, according to subsection b, a line with coordinates

$$u_i = a_{ij}x_j. \tag{3.10}$$

If we solve these equations for the x's in terms of the u's, and then substitute the result into

$$u_1x_1 + u_2x_2 + u_3x_3 = 0, \tag{3.11}$$

we obtain the equation of the conic in line coordinates:

$$\Phi[u_1,u_2,u_3] = \alpha_{ij}u_iu_j = 0, \tag{3.12}$$

where α_{ij} is the cofactor of a_{ij} in the determinant of the matrix $\{a_{ij}\}$. Thus, the conic is also *a curve of class 2*. In general, the order and the class of a curve are not identical. Plücker established general relations between order, class, and other characteristic numbers, such as the number of singularities on the curve. For non-singular curves the relation between order, n, and class, m, is n = m(m–1). Hence, the order typically grows much more rapidly than the class. Order and class have the same value for n=m=2.

d. *Circles, circular points at infinity*

So far the results obtained have had a pleasing duality between points and lines, but have not been terribly surprising. Consideration of a circle and its intersections with the ideal line provides unexpected answers.

Consider a circle in the affine plane

$$(x - a)^2 + (y - b)^2 = r^2. \tag{3.13}$$

Homogenize the expression as before to obtain

$$(x_1 - ax_3)^2 + (x_2 - bx_3)^2 = (rx_3)^2, \tag{3.14}$$

a "circle" in $\mathbf{P}^2$. Now consider the intersection of this circle with the line at infinity, i.e., with points for which $x_3 = 0$. The equation for such points is

$$x_1^2 + x_2^2 = 0. \tag{3.15}$$

There are two solutions, (1, i, 0) and (1, –i, 0), *regardless of* the parameters a, b and r of the circle. These two points, usually designated I and J, respectively, are called the *circular points at infinity.* All circles pass through these two points.

A line is called *isotropic* if it passes through a circular point at infinity. Thus, except for the line at infinity, [0,0,1], which passes through both I and J, isotropic lines have coordinates of the form $[u_1,u_2,u_3] = [1,\pm i,u_3]$.

e. *Foci*

An ellipse in the affine plane, situated and oriented appropriately, has the equation

$$\frac{x^2}{a^2} + \frac{y^2}{b^2} = 1, \tag{3.16}$$

with a>b. The two foci are at $(\pm c,0)$, where $c = \sqrt{a^2 - b^2}$. Homogenizing the equation for the ellipse we find

$$F(x_1,x_2,x_3) = \frac{x_1^2}{a^2} + \frac{x_2^2}{b^2} - x_3^2 = 0 \tag{3.17}$$

as the point equation in $\mathbb{P}^2$. Using the procedure outlined in subsections b and c we find the line equation to be

$$\Phi[u_1,u_2,u_3] = a^2u_1^2 + b^2u_2^2 - u_3^2 = 0. \tag{3.18}$$

As an illustration of this formalism we prove the result that *the product of the distances of the foci from a tangent is the same for all tangents* (and thus equal to the square of the minor axis of the ellipse): Let $u_1x + u_2y + u_3 = 0$ be a tangent to the ellipse. The distances of the foci from this line are $(\pm u_1c + u_3)/\sqrt{u_1^2 + u_2^2}$, respectively. The product of distances is then $(u_3^2 - u_1^2c^2)/(u_1^2 + u_2^2)$, which equals b^2 when $[u_1,u_2,u_3]$ satisfies (3.18). A similar argument holds for a hyperbola. It follows from replacing b by ib in the preceding.

We now inquire whether the ellipse has any isotropic tangents, i.e., whether $\Phi[1,\pm i,u_3] = 0$ can be satisfied for any choice of u_3. Substitution into the equation gives $u_3 = \pm c$. Thus, there are four isotropic tangents:

$$[\mathbf{t}_1] = [1,i,c];\ [\mathbf{t}_2] = [1,i,-c];\ [\mathbf{t}_3] = [1,-i,c];\ [\mathbf{t}_4] = [1,-i,-c]. \tag{3.19}$$

These four lines intersect pairwise in four points (besides I and J):

$$(\mathbf{x}_{13}) = (-c,\ 0,\ 1);\ (\mathbf{x}_{14}) = (0,\ ic,\ 1);\ (\mathbf{x}_{23}) = (0,\ -ic,\ 1);\ (\mathbf{x}_{24}) = (c,\ 0,\ 1). \tag{3.20}$$

We see that two of these points are in the affine plane, precisely at the focal points of the ellipse. This is a general result: *The focal points of a conic are the real intersections of the isotropic tangents.*

Let us write this out for the parabola: Start from $y = kx^2$; homogenize to $kx_1^2 - x_2x_3 = 0$. The line equation is: $u_1^2 - 4k\,u_2u_3 = 0$. There are two isotropic tangents, $[1,i,-\frac{i}{4k}]$ and $[1,-i,\frac{i}{4k}]$; the line at infinity is also a tangent. There is, thus, just one finite point of intersection, $(0,\frac{1}{4k},1)$, which, indeed, corresponds to the focus of the parabola in the affine plane.

In the general case, for a curve of class m, one defines the foci to be the intersections of the isotropic tangents. Except for degeneracies, there will be m^2 foci for such a curve. Of these m will be real and $m^2 - m$ complex.

In general, we must solve the equation $\Phi[1,\pm i,u_3] = 0$ to find the isotropic tangents. Assuming Φ is real, i.e., a polynomial in u_1,u_2,u_3 with real coefficients, we see that if $u_3 = -z = -(x + iy)$ is a solution of $\Phi[1,i,-z] = 0$, then $z^* = x - iy$ will solve $\Phi[1,-i,-z^*] = 0$. The intersection of the two lines $[1,i,-(x + iy)]$ and $[1,-i,-(x-iy)]$ is easily calculated to be $(x,y,1)$, a finite, real focus. All the real foci may be found in this way, and we have the result that *for a real equation of class m the foci in the affine plane, thought of as the complex z-plane, may be found from the equation*

$$\Phi[1,\ i,\ -z] = 0. \tag{3.21}$$

It is this result, due to Plücker, that Siebeck exploits in his theorem, since the challenge is now simply to write the equation for the roots/stagnation points in such a way that it can be reinterpreted as determining the foci of a curve of the appropriate class.

f. *Siebeck's theorem*

Returning to Eq.(2.2) we wish, then, to write P(z) in the form $\Phi[1,i,-z]$. We set

$$L_\alpha[u_1,u_2,u_3] = -x_\alpha u_1 - y_\alpha u_2 - u_3, \tag{3.22}$$

where the α'th vortex is at $x_\alpha + iy_\alpha$, so that $L_\alpha[1,i,-z] = z - z_\alpha$, and consider

$$\begin{aligned}\Phi[u_1,u_2,u_3] = \; & \Gamma_1 L_2[u_1,u_2,u_3]L_3[u_1,u_2,u_3] \ldots L_N[u_1,u_2,u_3] + \\ & \Gamma_2 L_1[u_1,u_2,u_3]L_3[u_1,u_2,u_3] \ldots L_N[u_1,u_2,u_3] + \ldots + \\ & \Gamma_N L_1[u_1,u_2,u_3]L_2[u_1,u_2,u_3] \ldots L_{N-1}[u_1,u_2,u_3] = 0.\end{aligned} \tag{3.23}$$

This polynomial is constructed such that the term with pre-factor Γ_α contains the product of all $L_\beta[\mathbf{u}]$ except $\beta=\alpha$. Clearly this is a polynomial equation in the u's of degree N–1, i.e., it defines a curve of class N–1. All coefficients are real (cf. (3.22)), so that the equation for the real, finite foci is

$$\Phi[1, i, -z] = P(z) = 0. \tag{3.24}$$

Thus, the stagnation points may be interpreted as the real foci of the curve given by (3.23).

Furthermore, the curve has all the lines connecting the vortices pairwise as tangents. For the line through vortices α and β has coordinates (cf. (3.6))

$$[\mathbf{u}_{\alpha\beta}] = [y_\alpha - y_\beta, -(x_\alpha - x_\beta), x_\alpha y_\beta - x_\beta y_\alpha], \tag{3.25}$$

and both

$$L_\alpha[\mathbf{u}_{\alpha\beta}] = -x_\alpha(y_\alpha - y_\beta) + y_\alpha(x_\alpha - x_\beta) - (x_\alpha y_\beta - x_\beta y_\alpha) \tag{3.26a}$$

and

$$L_\beta[\mathbf{u}_{\alpha\beta}] = -x_\beta(y_\alpha - y_\beta) + y_\beta(x_\alpha - x_\beta) - (x_\alpha y_\beta - x_\beta y_\alpha) \tag{3.26b}$$

vanish. Since every term in Φ contains at least one of these as a factor, it follows that

$$\Phi[\mathbf{u}_{\alpha\beta}] = 0 \tag{3.27}$$

for all pairs (α,β). All the lines connecting vortices pairwise are thus tangent to (3.23).

The points of tangency may be found from the developments in subsection b. We are instructed to differentiate Φ with respect to u_1, u_2, and u_3, and substitute the line coordinates, $[\mathbf{u}_{\alpha\beta}]$, for the tangent in question. Calculating $\partial\Phi/\partial u_1$ we note that we only need to differentiate the terms containing Γ_α and Γ_β – all the other terms will vanish when we substitute $[\mathbf{u}_{\alpha\beta}]$, since they will contain an undifferentiated factor L_α or L_β. We find:

$$\frac{\partial\Phi}{\partial u_1}[\mathbf{u}_{\alpha\beta}] = -(\Gamma_\alpha x_\beta + \Gamma_\beta x_\alpha) \prod_{\gamma\neq\alpha,\beta} L_\gamma[\mathbf{u}_{\alpha\beta}]; \tag{3.28a}$$

$$\frac{\partial \Phi}{\partial u_2}[\mathbf{u}_{\alpha\beta}] = -(\Gamma_\alpha y_\beta + \Gamma_\beta y_\alpha) \prod_{\gamma \neq \alpha,\beta} L_\gamma[\mathbf{u}_{\alpha\beta}]; \tag{3.28b}$$

$$\frac{\partial \Phi}{\partial u_3}[\mathbf{u}_{\alpha\beta}] = -(\Gamma_\alpha + \Gamma_\beta) \prod_{\gamma \neq \alpha,\beta} L_\gamma[\mathbf{u}_{\alpha\beta}]. \tag{3.28c}$$

Dividing out the common factor (the product of all L_γ with $\gamma \neq \alpha, \beta$ evaluated for the line coordinates $[\mathbf{u}_{\alpha\beta}]$ – this quantity is non-zero unless three vortices are on a line), we see that the point of tangency is the point

$$z_{\alpha\beta}^{(S)} = \frac{\Gamma_\alpha z_\beta + \Gamma_\beta z_\alpha}{\Gamma_\alpha + \Gamma_\beta} \tag{3.29}$$

in the affine plane. This is the stagnation point for the flow produced by the two vortices α and β ignoring all the others.

This completes the proof of Siebeck's theorem, which in our context reads: *The stagnation points of the flow induced by N point vortices on the infinite plane are the foci of the curve (3.23) of class N–1, that touches each line connecting two vortices at the stagnation point of the flow produced by these two vortices ignoring all others.*

We now turn to particular cases.

4. The case of three vortices

Let us first note that the case of two vortices is trivial. Siebeck's curve has the equation

$$(\Gamma_1 x_2 + \Gamma_2 x_1)u_1 + (\Gamma_1 y_2 + \Gamma_2 y_1)u_2 + (\Gamma_1 + \Gamma_2)u_3 = 0, \tag{4.1}$$

in line coordinates. This is the equation for the point (1.7), the coordinates of which appear as the coefficients of u_1, u_2, u_3, i.e., (4.1) is the equation for all lines passing through this point (a curve in line coordinates of class 1 corresponds to a curve in point coordinates of order 0). Alternatively, the stagnation point is determined by setting $[u_1, u_2, u_3] = [1, i, -z]$ in (4.1), which just gives the result (1.7).

The case of three vortices is considerably richer. We know that the stagnation points are the foci of a conic (a curve of class 2), and we need to choose coordinates that facilitate the discussion of this curve. Let the vortices be located at $z_\alpha = \xi_\alpha + i\eta_\alpha$, $\alpha = 1, 2, 3$; (here we use Greek letters for the cartesian coordinates of the vortices in order to avoid confusion with the coordinates x_1, x_2, and x_3 in $\mathbf{P}^2$). Assuming the vortices are not collinear, we may introduce new coordinates (X_1, X_2, X_3) in $\mathbf{P}^2$ via the equations

$$x_1 = \xi_1 X_1 + \xi_2 X_2 + \xi_3 X_3, \tag{4.2a}$$

$$x_2 = \eta_1 X_1 + \eta_2 X_2 + \eta_3 X_3, \tag{4.2b}$$

$$x_3 = X_1 + X_2 + X_3. \tag{4.2c}$$

Any finite point in $\mathbf{P}^2$, i.e., any point with $x_3 \neq 0$, will then have coordinates (X_1, X_2, X_3) with a sum that is different from zero. Since we are allowed to rescale, we choose to work with triples (X_1, X_2, X_3) that either have $X_1 + X_2 + X_3 = 1$, or that correspond to points on the line at infinity, i.e., have $X_1 + X_2 + X_3 = 0$. The benefit of this convention is that

(X_1,X_2,X_3) for a real triple may be interpreted as the *triangular coordinates* of a point in the plane based on the triangle spanned by the three vortices[3]. Thus, if a point P in the plane is connected to the vortices 1, 2 and 3, and the ratio of the areas of Δ23P, Δ31P, and Δ12P to Δ123 itself, all calculated as signed quantities depending on orientation, are denoted X_1, X_2 and X_3, respectively, we always have $X_1+X_2+X_3=1$. The construction is illustrated in Figure 1 for a case in which Δ12P, Δ23P and Δ123 (and thus X_1 and X_3) are all positive, whereas Δ31P (and thus X_2) is negative.

A point (ξ,η) in the affine plane corresponds to $(\xi,\eta,1)$ in $\mathbf{P}^2$, and has triangular coordinates

$$X_1 = \frac{\xi\eta_2-\xi_2\eta+\xi_2\eta_3-\xi_3\eta_2+\xi_3\eta-\xi\eta_3}{\xi_1\eta_2-\xi_2\eta_1+\xi_2\eta_3-\xi_3\eta_2+\xi_3\eta_1-\xi_1\eta_3}, \tag{4.3a}$$

$$X_2 = \frac{\xi_1\eta-\xi\eta_1+\xi\eta_3-\xi_3\eta+\xi_3\eta_1-\xi_1\eta_3}{\xi_1\eta_2-\xi_2\eta_1+\xi_2\eta_3-\xi_3\eta_2+\xi_3\eta_1-\xi_1\eta_3}, \tag{4.3b}$$

$$X_3 = \frac{\xi_1\eta_2-\xi_2\eta_1+\xi_2\eta-\xi\eta_2+\xi\eta_1-\xi_1\eta}{\xi_1\eta_2-\xi_2\eta_1+\xi_2\eta_3-\xi_3\eta_2+\xi_3\eta_1-\xi_1\eta_3}. \tag{4.3c}$$

There is a corresponding transformation of line coordinates:

$$U_1 = \xi_1u_1 + \eta_1u_2 + u_3, \tag{4.4a}$$

$$U_2 = \xi_2u_1 + \eta_2u_2 + u_3, \tag{4.4b}$$

$$U_3 = \xi_3u_1 + \eta_3u_2 + u_3, \tag{4.4c}$$

to ensure that $u_1x_1 + u_2x_2 + u_3x_3 = U_1X_1 + U_2X_2 + U_3X_3$.

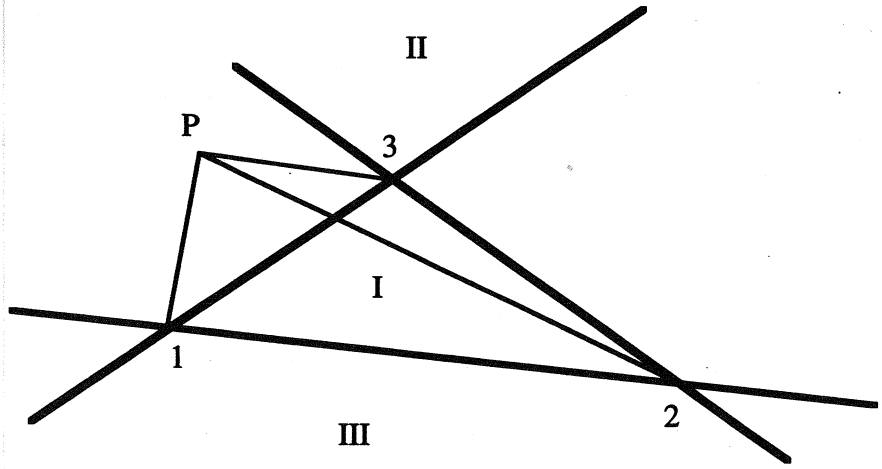

Figure 1: Illustration of the definition of triangular coordinates of an arbitrary point P relative to the vortex triangle 123. The regions I, II, and III, discussed in the text, are indicated.

The inverse transformation is

$$u_1 = \frac{U_1\eta_2-U_2\eta_1+U_2\eta_3-U_3\eta_2+U_3\eta_1-U_1\eta_3}{\xi_1\eta_2-\xi_2\eta_1+\xi_2\eta_3-\xi_3\eta_2+\xi_3\eta_1-\xi_1\eta_3}, \tag{4.5a}$$

$$u_2 = \frac{\xi_1U_2-\xi_2U_1+\xi_2U_3-\xi_3U_2+\xi_3U_1-\xi_1U_3}{\xi_1\eta_2-\xi_2\eta_1+\xi_2\eta_3-\xi_3\eta_2+\xi_3\eta_1-\xi_1\eta_3}, \tag{4.5b}$$

$$u_3 = \frac{(\xi_1\eta_2-\xi_2\eta_1)U_3+(\xi_2\eta_3-\xi_3\eta_2)U_1+(\xi_3\eta_1-\xi_1\eta_3)U_2}{\xi_1\eta_2-\xi_2\eta_1+\xi_2\eta_3-\xi_3\eta_2+\xi_3\eta_1-\xi_1\eta_3}. \tag{4.5c}$$

3) The treatise by Ferrers (1866) is concerned with trilinear and triangular coordinates and their geometrical applications; for an elementary discussion of applications of such coordinates in fluid mechanics see Aref (1992).

The line at infinity has coordinates $[U_1,U_2,U_3] = [1,1,1]$, and thus corresponds to the "unphysical" condition that $X_1+ X_2+ X_3 = 0$.

The triangular coordinates of the vortices are, of course, $(\mathbf{X}) = (1,0,0)$ for vortex 1; $(0,1,0)$ for 2; $(0,0,1)$ for 3. The line coordinates of the sides are $[\mathbf{U}] = [0,0,1]$ for the side 12; $[1,0,0]$ for 23; $[0,1,0]$ for 31. In these coordinates the expression for Φ simplifies considerably, as is seen by comparing (4.4) to (3.23). The line conic becomes

$$\Gamma_1U_2U_3 + \Gamma_2U_1U_3 + \Gamma_3U_1U_2 = 0. \tag{4.6}$$

Differentiating we find the point conic as follows:

$$X_1 = \Gamma_2U_3 + \Gamma_3U_2;\ \ X_2 = \Gamma_3U_1 + \Gamma_1U_3;\ \ X_3 = \Gamma_1U_2 + \Gamma_2U_1. \tag{4.7}$$

Solving these for the U's in terms of the X's gives

$$\begin{aligned} 2\Gamma_2\Gamma_3U_1 &= -\Gamma_1X_1 + \Gamma_2X_2 + \Gamma_3X_3;\\ 2\Gamma_3\Gamma_1U_2 &= \ \Gamma_1X_1 - \Gamma_2X_2 + \Gamma_3X_3;\\ 2\Gamma_1\Gamma_2U_3 &= \ \Gamma_1X_1 + \Gamma_2X_2 - \Gamma_3X_3. \end{aligned} \tag{4.8}$$

Substituting these expressions in the equation for the line conic gives the equation for the point conic in area coordinates:

$$(\Gamma_1X_1)^2 + (\Gamma_2X_2)^2 + (\Gamma_3X_3)^2 = 2\Gamma_1\Gamma_2X_1X_2 + 2\Gamma_2\Gamma_3X_2X_3 + 2\Gamma_3\Gamma_1X_3X_1. \tag{4.9}$$

This equation may also be written

$$\begin{aligned} &(\sqrt{\Gamma_1X_1} + \sqrt{\Gamma_2X_2} + \sqrt{\Gamma_3X_3})(\sqrt{\Gamma_1X_1} + \sqrt{\Gamma_2X_2} - \sqrt{\Gamma_3X_3})\times\\ &(\sqrt{\Gamma_1X_1} - \sqrt{\Gamma_2X_2} + \sqrt{\Gamma_3X_3})(-\sqrt{\Gamma_1X_1} + \sqrt{\Gamma_2X_2} + \sqrt{\Gamma_3X_3}) = 0, \end{aligned} \tag{4.10}$$

i.e, as

$$\sqrt{\Gamma_1X_1} \pm \sqrt{\Gamma_2X_2} \pm \sqrt{\Gamma_3X_3} = 0. \tag{4.11}$$

The points of tangency with the triangle spanned by the vortices are

$$\begin{aligned} (\mathbf{X}_{23}) &= \left(0, \frac{\Gamma_3}{\Gamma_2+\Gamma_3}, \frac{\Gamma_2}{\Gamma_2+\Gamma_3}\right);\\ (\mathbf{X}_{31}) &= \left(\frac{\Gamma_3}{\Gamma_3+\Gamma_1}, 0, \frac{\Gamma_1}{\Gamma_3+\Gamma_1}\right);\\ (\mathbf{X}_{12}) &= \left(\frac{\Gamma_2}{\Gamma_1+\Gamma_2}, \frac{\Gamma_1}{\Gamma_1+\Gamma_2}, 0\right). \end{aligned} \tag{4.12}$$

We see that the three lines,

$$\Gamma_1X_1 = \Gamma_2X_2 = \Gamma_3X_3, \tag{4.13}$$

or, in line coordinates,

$$[\mathbf{U}] = [\Gamma_1,-\Gamma_2, 0];\ \ [-\Gamma_1, 0, \Gamma_3];\ \ [0, \Gamma_2,-\Gamma_3], \tag{4.13'}$$

connect the vortices to the points of tangency on the opposite sides (4.12). They are concurrent in the point T with coordinates

$$\left(X_1^{(T)}, X_2^{(T)}, X_3^{(T)}\right) = (\Gamma_2\Gamma_3, \Gamma_3\Gamma_1, \Gamma_1\Gamma_2)/(\Gamma_1\Gamma_2 + \Gamma_2\Gamma_3 + \Gamma_3\Gamma_1), \tag{4.14}$$

(which is at infinity if the harmonic mean of the vortex strengths vanishes).

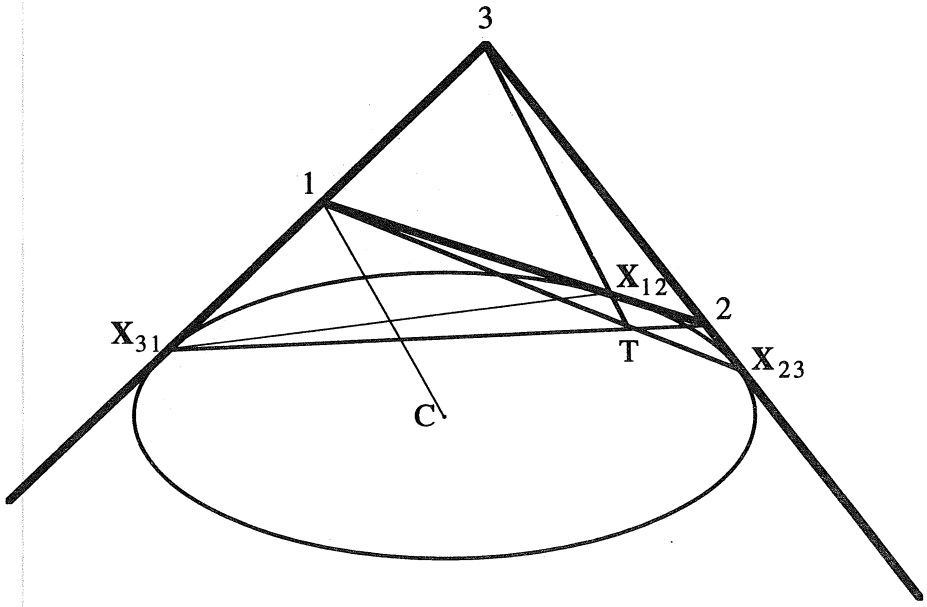

Figure 2: Relative situation of vortices (1, 2 and 3), Siebeck's conic with center C, the three points of tangency, X_{12}, X_{23}, X_{31}, and the point of concurrency, T, of $1X_{23}$, $2X_{31}$, and $3X_{12}$. The lines 1C, 2C and 3C bisect $X_{31}X_{12}$, $X_{12}X_{23}$, and $X_{23}X_{31}$, respectively.

The conic (4.9) is, except for a change in notation, the same as was considered in an earlier analysis of three-vortex motion (see Aref, 1979, Eq.(14)). It follows, therefore, that the classification of the nature of the conic that has the stagnation points as foci in terms of the values of the vortex strengths is exactly the classification of the motion itself found in the earlier work[4]. In particular, the stagnation point conic is

$$\begin{aligned} &\textit{an ellipse if} && \Gamma_1\Gamma_2\Gamma_3\,(\Gamma_1+\Gamma_2+\Gamma_3) > 0; \\ &\textit{a parabola if} && \Gamma_1+\Gamma_2+\Gamma_3 = 0; \\ &\textit{a hyperbola if} && \Gamma_1\Gamma_2\Gamma_3\,(\Gamma_1+\Gamma_2+\Gamma_3) < 0. \end{aligned} \tag{4.15}$$

The type of this conic depends only on the vortex strengths, and thus is invariant in time (except for the degeneracy that occurs when the vortices are on a line and the conic collapses to a line segment). Indeed, the equation of the inscribed conic in triangular coordinates, (4.9), is invariant with respect to the shape of the vortex triangle, and thus *a fortiori* the classification, (4.15), of whether it is an ellipse, a parabola or a hyperbola will be invariant with respect to the evolution of that triangle in time as the motion unfolds.

4) The formal way to decide this is to write out the coefficient matrix of the quadratic (4.9), convert back to variables x_1, x_2, x_3 via (4.2) and consider the determinant of the appropriate minor (cf. the text following Eq.(3.19)).

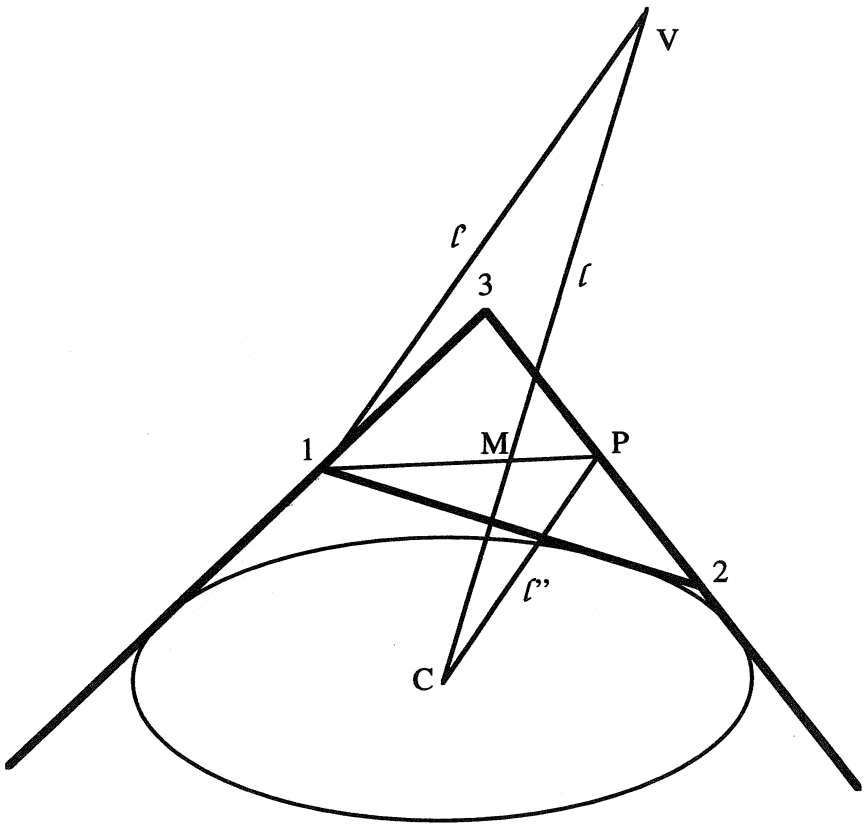

Figure 3: Geometry of the midpoint, M, center of vorticity, V, and center of Siebeck's conic, C. Note that M, V and C are collinear and CM:MV = 1:2. Thus, ΔMPC is similar to ΔM1V, the lines CP and 1V being parallel.

Our results thus far establish several qualitative differences between the two elliptic, the parabolic and the hyperbolic cases regarding the location of stagnation points. We divide the plane into regions according to the lines connecting the vortices pairwise. Without loss of generality we may restrict consideration to the case $\Gamma_1 \geq \Gamma_2 > 0$, since other choices of signs follow by re-labelling of indices and/or by reflection in the flow plane. Then, in Fig.1, the stagnation points in the elliptic cases will either both be in region I (when $\Gamma_3 > 0$), or will both be in region III (when $\Gamma_3 < 0$) since the ellipse will be situated in one of these two regions (see Fig.2 for an example of the $\Gamma_3 < 0$ case). In the hyperbolic case there will be one stagnation point in region II and one in region III since the hyperbola will have a branch in each of these two regions. Thus, in the hyperbolic case, so long as the vortices are not collinear, there must always be two distinct stagnation points, whereas in the elliptic case the two stagnation points can coincide when the ellipse degenerates to a circle (criteria for when this happens are developed below). In the parabolic case, the single stagnation point will always be in region III since this is where the parabola will be located. This immediate consequence of the geometric characterization of stagnation points is considerably less transparent if one simply proceeds with finding the roots of the polynomial (2.2) algebraically. For the case of positive vortex strengths the Gauss-Lucas theorem (cf. Marden, 1949, Ch.II) implies that the stagnation points must lie within the triangle spanned by the vortices. The location as foci of an inscribed ellipse is clearly much sharper.

In the elliptic and hyperbolic case let the triangular coordinates of the two stagnation points be (X_1,X_2,X_3) and $(\tilde{X}_1,\tilde{X}_2,\tilde{X}_3)$, respectively. From (2.8) we deduce that

$$X_1+\tilde{X}_1=\frac{\Gamma_2+\Gamma_3}{\Gamma_1+\Gamma_2+\Gamma_3};\ X_2+\tilde{X}_2=\frac{\Gamma_3+\Gamma_1}{\Gamma_1+\Gamma_2+\Gamma_3};\ X_3+\tilde{X}_3=\frac{\Gamma_1+\Gamma_2}{\Gamma_1+\Gamma_2+\Gamma_3}. \quad (4.16)$$

Thus, the center of the conic in Siebeck's theorem has triangular coordinates

$$\left(X_1^{(C)}, X_2^{(C)}, X_3^{(C)}\right)=\left(\frac{\Gamma_2+\Gamma_3}{2(\Gamma_1+\Gamma_2+\Gamma_3)}, \frac{\Gamma_3+\Gamma_1}{2(\Gamma_1+\Gamma_2+\Gamma_3)}, \frac{\Gamma_1+\Gamma_2}{2(\Gamma_1+\Gamma_2+\Gamma_3)}\right). \quad (4.17)$$

These coordinates are again invariant both with respect to the actual configuration of the vortices (shape of the triangle) and with respect to the motion. It is easy to verify that the line connecting vortex 1 to the center, C, bisects the line connecting the points of tangency $(\mathbf{X}_{31})$ and $(\mathbf{X}_{12})$, with corresponding results by permutation of indices. Figure 2 summarizes the relative situation and role of the points of tangency, and the points T and C introduced thus far. It is important not to confuse the point T (point of concurrency of lines connecting vortices to points of tangency) and the point C (center of Siebeck's conic).

Since C, the center of Siebeck's conic, is situated at the midpoint of the line joining the two stagnation points, we note from (2.9) that this point must be on the line through the centroid of the vortex configuration and the center of vorticity. Alternatively, we may note that the line $[\mathbf{U}] = [\Gamma_2-\Gamma_3,\Gamma_3-\Gamma_1,\Gamma_1-\Gamma_2]$ passes through the centroid, $(\mathbf{X}) = (1,1,1)$, the center of vorticity, $(\Gamma_1,\Gamma_2,\Gamma_3)/(\Gamma_1+\Gamma_2+\Gamma_3)$, and the point C, Eq.(4.17). Designating the complex position of C by $z^{(C)}$, and recalling our earlier definitions of z_m and z_c (see §2), we have:

$$z^{(C)} = \tfrac{3}{2}z_m - \tfrac{1}{2}z_c. \quad (4.18)$$

This relation shows, further, that the centroid splits the line segment connecting the center of the conic to the center of vorticity in the ratio 1:2. Since the centroid itself splits each median in the vortex triangle in this ratio, the following construction of the point C presents itself (Fig.3): From the instantaneous vortex triangle construct the centroid as the point of concurrency of its medians. From the vortex positions and the vortex strengths determine the center of vorticity. Draw the line, ℓ, through the centroid and the center of vorticity (this is $[\Gamma_2-\Gamma_3,\Gamma_3-\Gamma_1,\Gamma_1-\Gamma_2]$ – we list the coordinates so that the construction can be verified algebraically). Join any vortex, e.g., 1 as shown in Fig. 3, to the center of vorticity, producing a line ℓ' (coordinates: $[0,-\Gamma_3,\Gamma_2]$). Through the midpoint of the opposite side in the vortex triangle (coordinates: (0,1,1)) draw the line ℓ'' parallel to ℓ' (in this case parallel to $[0,-\Gamma_3,\Gamma_2]$ – this gives the line $[\Gamma_2-\Gamma_3,\Gamma_2+\Gamma_3,-(\Gamma_2-\Gamma_3)]$; 'parallelism' in triangular coordinates means that these two lines intersect on the line [1,1,1]). The point C is then found at the intersection of ℓ and ℓ'' (i.e., at the intersection of $[\Gamma_2-\Gamma_3,\Gamma_3-\Gamma_1,\Gamma_1-\Gamma_2]$ and $[\Gamma_2-\Gamma_3,\Gamma_2+\Gamma_3,-(\Gamma_2-\Gamma_3)]$, as is easily verified).

From the result on the product of the distances of the foci from a tangent (see §3, subsection e, following (3.18)) we have

$$\frac{X_1\hat{X}_1}{d_{23}^2} = \frac{X_2\hat{X}_2}{d_{31}^2} = \frac{X_3\hat{X}_3}{d_{12}^2}, \tag{4.19}$$

where d_{12}, d_{23} and d_{31} are the lengths of the sides of the triangle (using an obvious notation). The common value of the expressions in (4.19) is positive in the elliptic case and negative in the hyperbolic case. Combining (4.16) and (4.19) we see that the triangular coordinates of the stagnation points of three vortices must solve the system of equations

$$\begin{aligned}
&\frac{1}{d_{23}^2}\{(\Gamma_1+\Gamma_2+\Gamma_3)X_1-(\Gamma_2+\Gamma_3)\}X_1 = \\
&\frac{1}{d_{31}^2}\{(\Gamma_1+\Gamma_2+\Gamma_3)X_2-(\Gamma_3+\Gamma_1)\}X_2 = \\
&\frac{1}{d_{12}^2}\{(\Gamma_1+\Gamma_2+\Gamma_3)X_3-(\Gamma_1+\Gamma_2)\}X_3,
\end{aligned} \tag{4.20}$$

with

$$X_1 + X_2 + X_3 = 1. \tag{4.20'}$$

Ferrers (1866, Ch.VI §33) finds equations equivalent to (4.20) using the theory of reciprocal polars.)

In the parabolic case the first term in the curly brackets in (4.20) vanishes, and for the single stagnation point we have simply[5]

$$\Gamma_1X_1 = k\, d_{23}^2;\ \Gamma_2X_2 = k\, d_{31}^2;\ \Gamma_3X_3 = k\, d_{12}^2. \tag{4.21}$$

Here k is the common value of the expressions in (4.20), and we have used that the vortex strengths sum to zero. Multiplying by $\Gamma_2\Gamma_3$, $\Gamma_3\Gamma_1$, $\Gamma_1\Gamma_2$, respectively, adding and using (4.20') we obtain:

$$k = \frac{\Gamma_1\Gamma_2\Gamma_3}{\Gamma_1\Gamma_2 d_{12}^2 + \Gamma_2\Gamma_3 d_{23}^2 + \Gamma_3\Gamma_1 d_{31}^2}. \tag{4.22}$$

Thus, the triangular coordinates of the stagnation point in this case are

$$(X_1^{(S)}, X_2^{(S)}, X_3^{(S)}) = \frac{(\Gamma_2\Gamma_3 d_{23}^2, \Gamma_3\Gamma_1 d_{31}^2, \Gamma_1\Gamma_2 d_{12}^2)}{\Gamma_1\Gamma_2 d_{12}^2 + \Gamma_2\Gamma_3 d_{23}^2 + \Gamma_3\Gamma_1 d_{31}^2}. \tag{4.23}$$

We notice that the denominator is a constant of the motion (cf. Aref, 1979). Hence, we have the result that *in the parabolic case the triangular coordinates of the stagnation point, each scaled by the square of the corresponding side in the vortex triangle, are constant during the motion.*[6] This result strikes us as being quite remarkable, since the

5) One might worry that (4.21) arises from (4.20) by using (4.16), and this condition is ambiguous when one focus is at infinity. However, an independent derivation shows that (4.21) are, indeed, the correct equations for the focus in the parabolic case.

6) When the denominator in (4.23) vanishes, there is no finite stagnation point, as may also be seen from the explicit solution that is available for this case (Rott 1989; Aref 1989).

stagnation point is not invariant in an Eulerian or Lagrangian sense, and does not, in general, have a fixed position relative to the vortices.

Another way to state the result (4.23) arises from the expressions $X_1^{(S)} = h_1^{(S)} d_{23}/2\Delta$, etc., where $h_1^{(S)}$ denotes the distance of the stagnation point from the side 23. Substituting this form for the triangular coordinates into (4.23), we obtain

$$\left(\frac{h_1^{(S)}}{d_{23}}, \frac{h_2^{(S)}}{d_{31}}, \frac{h_3^{(S)}}{d_{12}}\right) = \frac{2\Delta\,(\Gamma_2\Gamma_3, \Gamma_3\Gamma_1, \Gamma_1\Gamma_2)}{\Gamma_1\Gamma_2 d_{12}^2 + \Gamma_2\Gamma_3 d_{23}^2 + \Gamma_3\Gamma_1 d_{31}^2}. \tag{4.24}$$

Hence, (4.23) implies that the dimensionless ratio of the distance of the stagnation point from a side to the length of that side varies proportionally to the vortex triangle area.

It is not difficult to show (cf. Ferrers, 1866, Art.6) that the equation for the circumscribed circle of the vortex triangle is

$$d_{12}^2 X_1 X_2 + d_{23}^2 X_2 X_3 + d_{31}^2 X_3 X_1 = 0. \tag{4.25}$$

We see that the stagnation point (4.23) is situated on this circle.

In the elliptic and hyperbolic cases we need to consider the full quadratic equations (4.20) to determine the triangular coordinates of the two stagnation points. Setting the common value of the expression (4.20) to $-k(\Gamma_1+\Gamma_2+\Gamma_3)$, we find

$$\begin{aligned} X_1 &= X_1^{(C)} \pm \sqrt{\left(X_1^{(C)}\right)^2 - k d_{23}^2}, \\ X_2 &= X_2^{(C)} \pm \sqrt{\left(X_2^{(C)}\right)^2 - k d_{31}^2}, \\ X_3 &= X_3^{(C)} \pm \sqrt{\left(X_3^{(C)}\right)^2 - k d_{12}^2}. \end{aligned} \tag{4.26}$$

Thus

$$\pm\sqrt{\left(X_1^{(C)}\right)^2 - k d_{23}^2} \pm \sqrt{\left(X_2^{(C)}\right)^2 - k d_{31}^2} \pm \sqrt{\left(X_3^{(C)}\right)^2 - k d_{12}^2} = 0. \tag{4.27}$$

This equation is of the form (4.11). Hence, squaring twice we obtain an equation of the form (4.9) regardless of the combination of signs used in (4.27). This equation is

$$\begin{aligned} &k^2\left(d_{12}^4 + d_{23}^4 + d_{31}^4 - 2d_{12}^2 d_{23}^2 - 2d_{23}^2 d_{31}^2 - 2d_{31}^2 d_{12}^2\right) - \\ &\quad 2k\,[\,d_{12}^2\left\{\left(X_3^{(C)}\right)^2 - \left(X_1^{(C)}\right)^2 - \left(X_2^{(C)}\right)^2\right\} + d_{23}^2\left\{\left(X_1^{(C)}\right)^2 - \left(X_2^{(C)}\right)^2 - \left(X_3^{(C)}\right)^2\right\} + \\ &\qquad d_{31}^2\left\{\left(X_2^{(C)}\right)^2 - \left(X_3^{(C)}\right)^2 - \left(X_1^{(C)}\right)^2\right\}\,] + \\ &\left(X_1^{(C)}\right)^4 + \left(X_2^{(C)}\right)^4 + \left(X_3^{(C)}\right)^4 - 2\left(X_1^{(C)}\right)^2\left(X_2^{(C)}\right)^2 - 2\left(X_2^{(C)}\right)^2\left(X_3^{(C)}\right)^2 - 2\left(X_3^{(C)}\right)^2\left(X_1^{(C)}\right)^2 = 0. \end{aligned} \tag{4.28}$$

The coefficient of k^2 is $(4\Delta)^2$ by Hero's formula for the area of a triangle. The constant term can be simplified to $-\Gamma_1\Gamma_2\Gamma_3/(\Gamma_1+\Gamma_2+\Gamma_3)^3$. The coefficient of k is

$$-\{\,d_{12}^2(\Gamma_1\Gamma_2 - \Gamma_3\Sigma) + d_{23}^2(\Gamma_2\Gamma_3 - \Gamma_1\Sigma) + d_{31}^2(\Gamma_3\Gamma_1 - \Gamma_2\Sigma)\,\}/\Sigma^2, \tag{4.29}$$

where the shorthand $\Sigma = \Gamma_1 + \Gamma_2 + \Gamma_3$ has been used.

It is clear from these equations – even without pausing to sort out the signs in (4.26) – that k, in general, will be a function of the vortex separations that is not dynamically invariant. Indeed, it is easy to see that the only combinations of Γ_1, Γ_2, Γ_3 for which (4.29) is a constant of the motion are $\Gamma_1 = \Gamma_2 = \pm\,\Gamma_3$ (and even in these cases k depends on the vortex triangle area Δ). Hence, we do not expect a counterpart of the similarity law (4.23) in the general case.

5. Streamline topology

The instantaneous streamline pattern of the flow is determined by the location of the vortices and by the stagnation points. The latter are the points at which streamlines intersect. For the case of two point vortices it is not difficult to see that the flow topology must be invariant as the motion proceeds. For the location of the vortices and the stagnation point simply rotate rigidly about the center of vorticity, and so the entire streamline configuration must also rotate about this point.

For two vortices, with the sum of their circulations different from zero, there are three possible streamline topologies with a single stagnation point, as indicated in Fig.3.

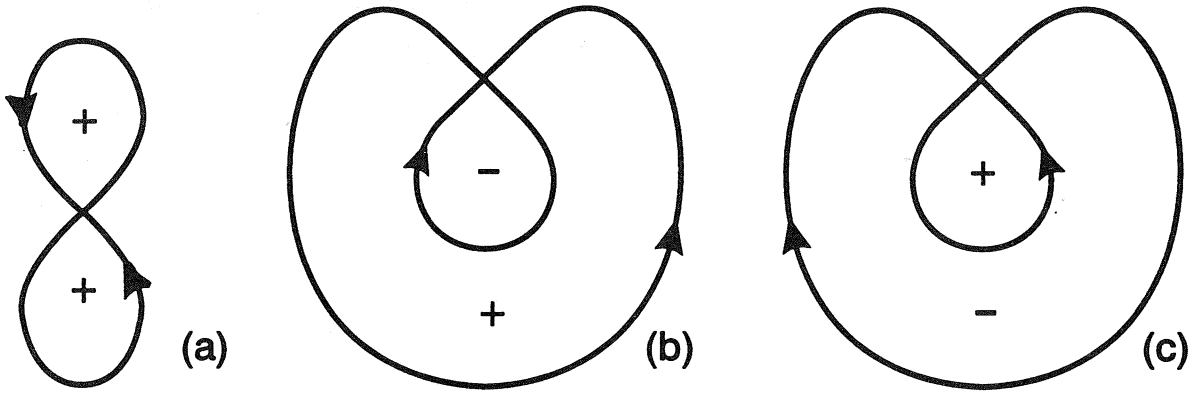

Figure 3: Streamline topology for the flow about two vortices with non-zero net circulation. There is one stagnation point. Flow about (a) two positive vortices; (b) a vortex of either sign with the sum of strengths positive; (c) a vortex of either sign with the sum of strengths negative.

5.1 *Streamline topologies for three vortices*

For three vortices the situation is richer. The vortices move relative to one another, and a stagnation point will move relative to the vortices. The nature of the stagnation point as a fixed point of the flow is clear enough, however: Since it is in a potential flow, the two intersecting streamlines at a stagnation must always form a right angle.

Let us first consider the elliptic and hyperbolic cases for which there are two stagnation points. Since the sum of the vortex strengths is different from zero, the far-field velocity at any instant is like the flow due to a single vortex of strength equal to this sum. In particular, no streamlines go off to infinity. It then follows that the streamlines must form a

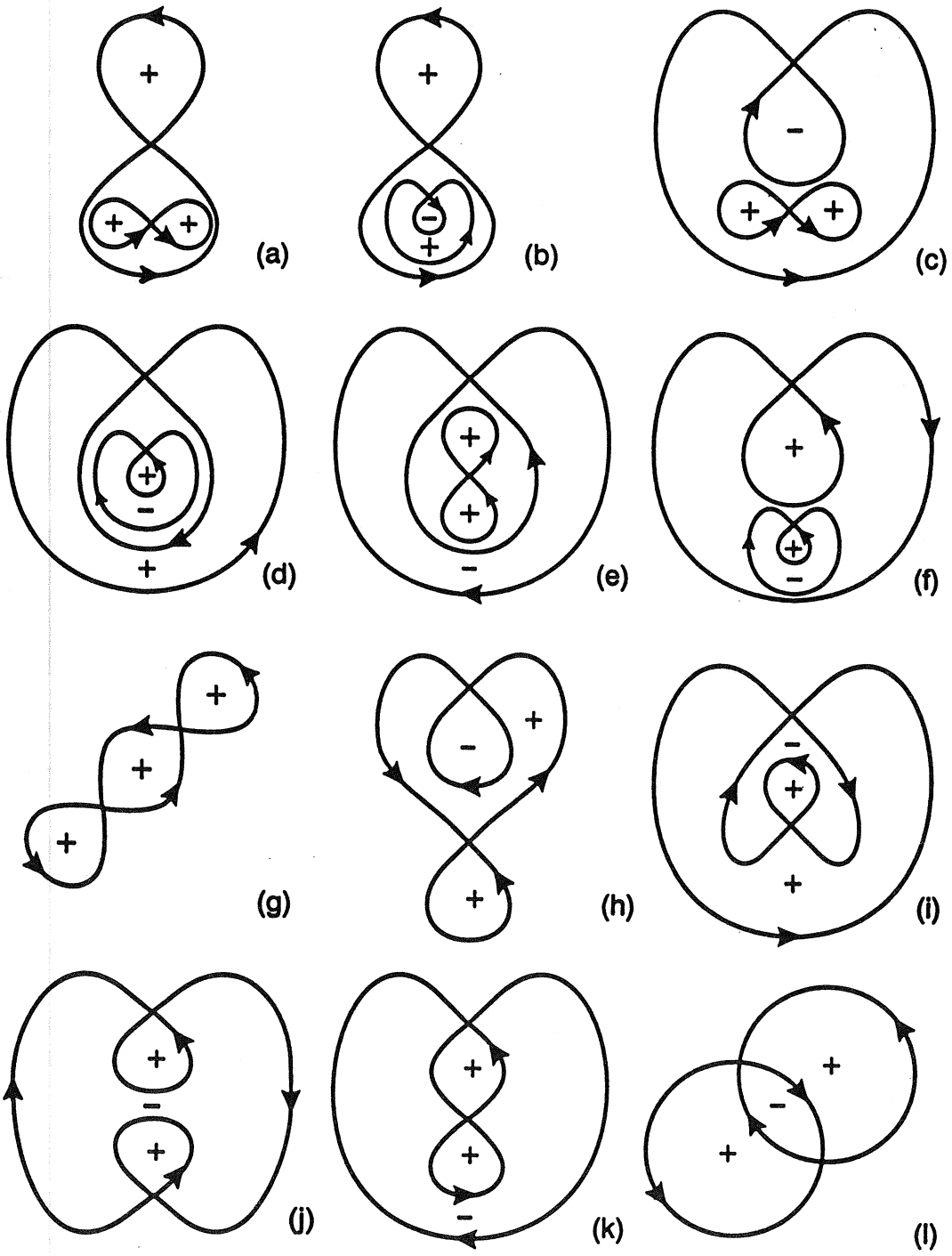

Figure 4: Streamline topology for flow about three vortices with non-zero net circulation, $\Gamma_1+\Gamma_2+\Gamma_3 \neq 0$. The derivation of the different cases is discussed in the text. Patterns (a)-(f) have no heteroclinic loops and are the 'generic' cases. Patterns (g)-(k) have one heteroclinic loop, (l) has three. Streamline topologies a, e, f, g, j, and k are for the elliptic cases; b, c, d, h, i, l are for the hyperbolic case.

pattern in which the two stagnation points are connected, either to themselves or to each other, and a simple enumeration of the topological possibilities accounts for the different types of flow.

Borrowing from the dynamical systems nomenclature we designate a streamline loop connecting a stagnation point to itself as a *homoclinic loop,* and we designate two streamline segments connecting two stagnation points as a *heteroclinic loop.* Heteroclinic loops occur only if the streamfunction of the flow takes the same value at both stagnation points. This will not generally be the case, and so signifies a special vortex configuration at which a bifurcation of the streamline pattern takes place. The typical streamline topology will consist solely of homoclinic loops.

In order to find these, we return to Fig.3 and consider the pattern 3(a) or 3(b) to be 'substituted' for either positive vortex in 3(a). This gives the streamline topologies in Fig.4(a),(b). In generating from Fig.3(b) a possible streamline topology for three vortices our sign convention dictates that the pattern 3(a) can be substituted for the positive vortex, leading to Fig.4(c), but not the pattern 3(b), since that would produce a pattern with two negative vortices. However, the pattern 3(c) can be substituted for the negative vortex in 3(b) leading to Fig.4(d). Again, in Fig.3(c) we may substitute 3(a) for the positive vortex, producing Fig.4(e), or 3(c) for the negative vortex, producing Fig.4(f). All these configurations have four homoclinic loops, and exhaust the possibilities for patterns with all homoclinic loops.

If we start from Fig.3(a) and somewhere along either homoclinic loop 'pinch off' a new homoclinic loop, we produce the streamline topologies in Figs.4(g) and (h) depending on whether the 'pinched off' loop is outside or inside one of the existing homoclinic loops. A similar transformation applied to Fig.3(b) – where we are only allowed to place a loop outside the positive vortex loop or inside the negative vortex loop, since we otherwise would produce a second negative vortex – yields Fig.4(i) and a repeat of Fig.4(h). From Fig.3(c) we similarly produce Figs.4(j) and (k). All these configurations have two homoclinic loops and one heteroclinic loop. Conversely, by letting a homoclinic loop in Figs.4(g-k) shrink to a point (if allowed by the presence of the remaining two vortices) we reproduce one of the streamline topologies from Fig.3. Finally, Fig.4(l) shows the single possibility when there are no homoclinic loops. These 12 streamline patterns are the only ones possible for three vortices on the infinite plane when the sum of strengths is non-zero. By considering the sense of the far-field flow in these diagrams we see that Figs.4(a,e,f,g,j,k) correspond to elliptic cases, whereas Figs.4(b,c,d,h,i,l) correspond to hyperbolic cases.

There are four degenerate cases in which there is only a single stagnation point, where three streamline branches divide the plane into six sectors each of opening angle $\pi/3$. They can be determined by drawing the three streamline segments close to the degenerate stagnation point, and then connecting these segments to form loops in all possible ways (consistent with our sign convention on vortex strengths). The resulting four patterns are shown in Fig.5.

There is a simple algebraic condition, which follows from Eqs.(4.16) and (4.18), for when such degeneracy occurs. In the elliptic case the stagnation points can coincide without the vortices becoming collinear, because Siebeck's conic – which is an ellipse in this case – can degenerate to a circle. Thus, setting $(X_1,X_2,X_3) = (\tilde{X}_1,\tilde{X}_2,\tilde{X}_3) = \left(X_1^{(C)}, X_2^{(C)}, X_3^{(C)}\right)$, we find the condition

$$\left(\frac{\Gamma_2+\Gamma_3}{d_{23}}\right)^2 = \left(\frac{\Gamma_3+\Gamma_1}{d_{31}}\right)^2 = \left(\frac{\Gamma_1+\Gamma_2}{d_{12}}\right)^2, \tag{5.1}$$

which determines the shape of the vortex triangle. Since $\Gamma_1+\Gamma_3$ and $\Gamma_2+\Gamma_3$ are of the same sign in this case, (5.1) may be written

$$\frac{\Gamma_2+\Gamma_3}{d_{23}} = \frac{\Gamma_3+\Gamma_1}{d_{31}} = \pm\frac{\Gamma_1+\Gamma_2}{d_{12}}, \tag{5.2}$$

where the sign in the last term is the sign of Γ_3. Thus, if the vortices form an equilateral triangle, the two stagnation points will coincide if $\Gamma_1=\Gamma_2=\Gamma_3$, but also if $\Gamma_1:\Gamma_2:\Gamma_3 = 1:1:(-3)$. In the former case we get the streamline pattern Fig.5(a), in the latter Fig.5(d).

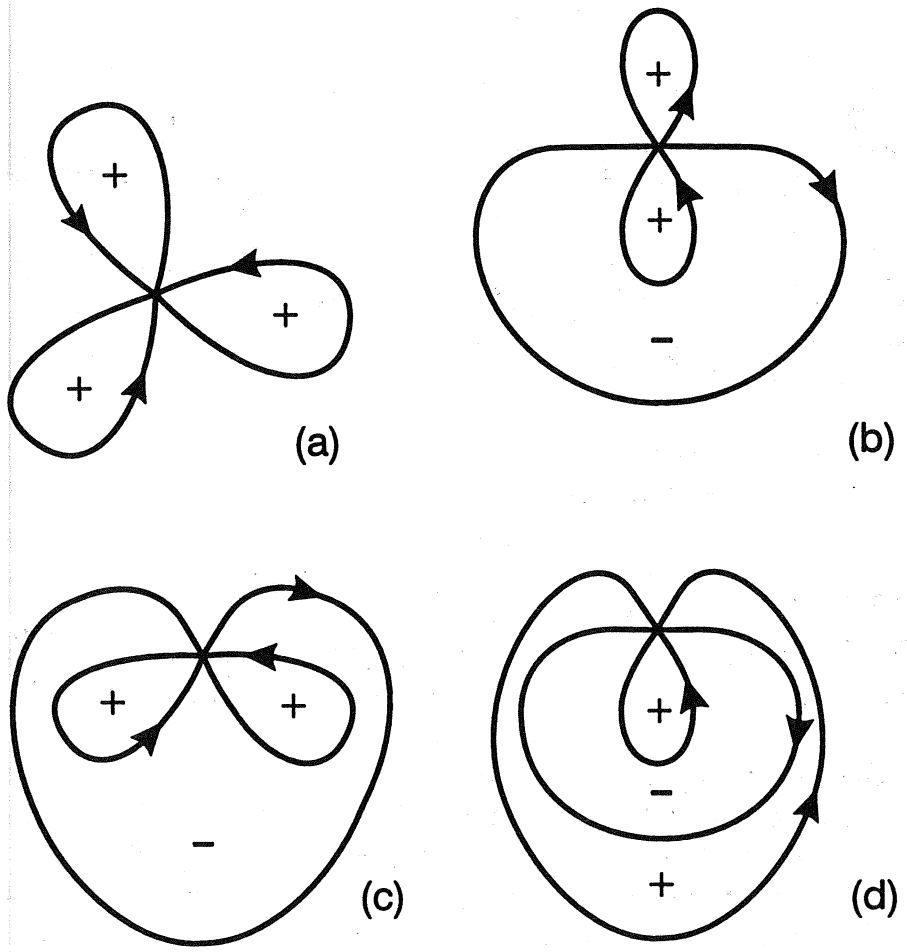

Figure 5: Streamline topology for flow about three vortices with non-zero net circulation, $\Gamma_1+\Gamma_2+\Gamma_3 \neq 0$ in the degenerate cases with a single stagnation point.

In the hyperbolic case the two stagnation points (alias foci of a hyperbola) can only coincide if the vortices are collinear. Hence, the patterns in Fig.5(b) and (d) must arise from collinear vortices. In particular, in the collinear state the negative vortex 3 must always be situated between the positive vortices 1 and 2 in order for a degenerate stagnation point to arise.

The streamline patterns for the parabolic case can be thought of as limiting forms of the elliptic patterns in Fig.4(e), (f), (j) and (k). These four forms are shown in Fig.6.

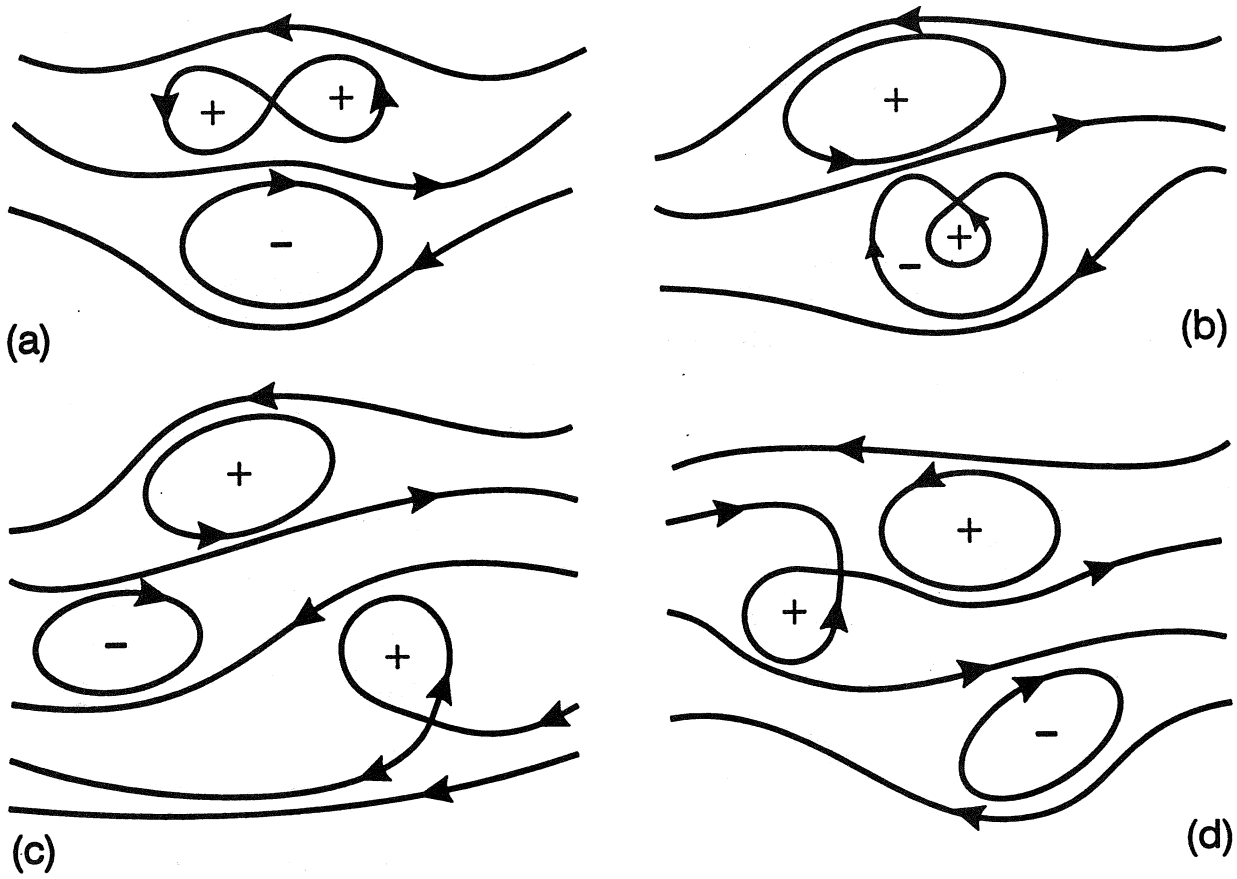

Figure 6: Streamline topology for flow about three vortices with zero net circulation, $\Gamma_1+\Gamma_2+\Gamma_3 = 0$, in which case there is a single stagnation point.

In all cases it must be kept in mind that the diagrams of Figs.4-6 give the possible streamline topologies without regard to scale (and the angles that arise between streamline branches at a stagnation point must be $\pi/2$). When actual values are substituted for the vortex strengths, and the diagrams are accurately constructed, the relative size of the various loops may be quite different from what is shown in Figs.4-6. We have plotted some correctly scaled streamline patterns for given vortex strengths in Fig.7.

The construction of the different streamline topologies assures that all the topologies identified in Figs.4-6 will actually occur for suitable choices of vortex positions and strengths. Indeed, it should be possible to produce all of them with the three vortices situated on a line. However, predicting the positions and strengths of three vortices to produce a given pattern is not a simple matter, and some patterns are found much more readily than others.

5.2 *Change of streamline topology*

It is natural to inquire into the dynamical conditions under which the streamline topology either is invariant or changes during the motion of the three vortices. This question is of some interest, as we shall see, although the physical relevance of the answer

is not particularly clear, since an instantaneous streamline is not a material curve. A general discussion seems difficult and we are content to consider the special cases $\Gamma_1 = \Gamma_2 = \pm \Gamma_3$.

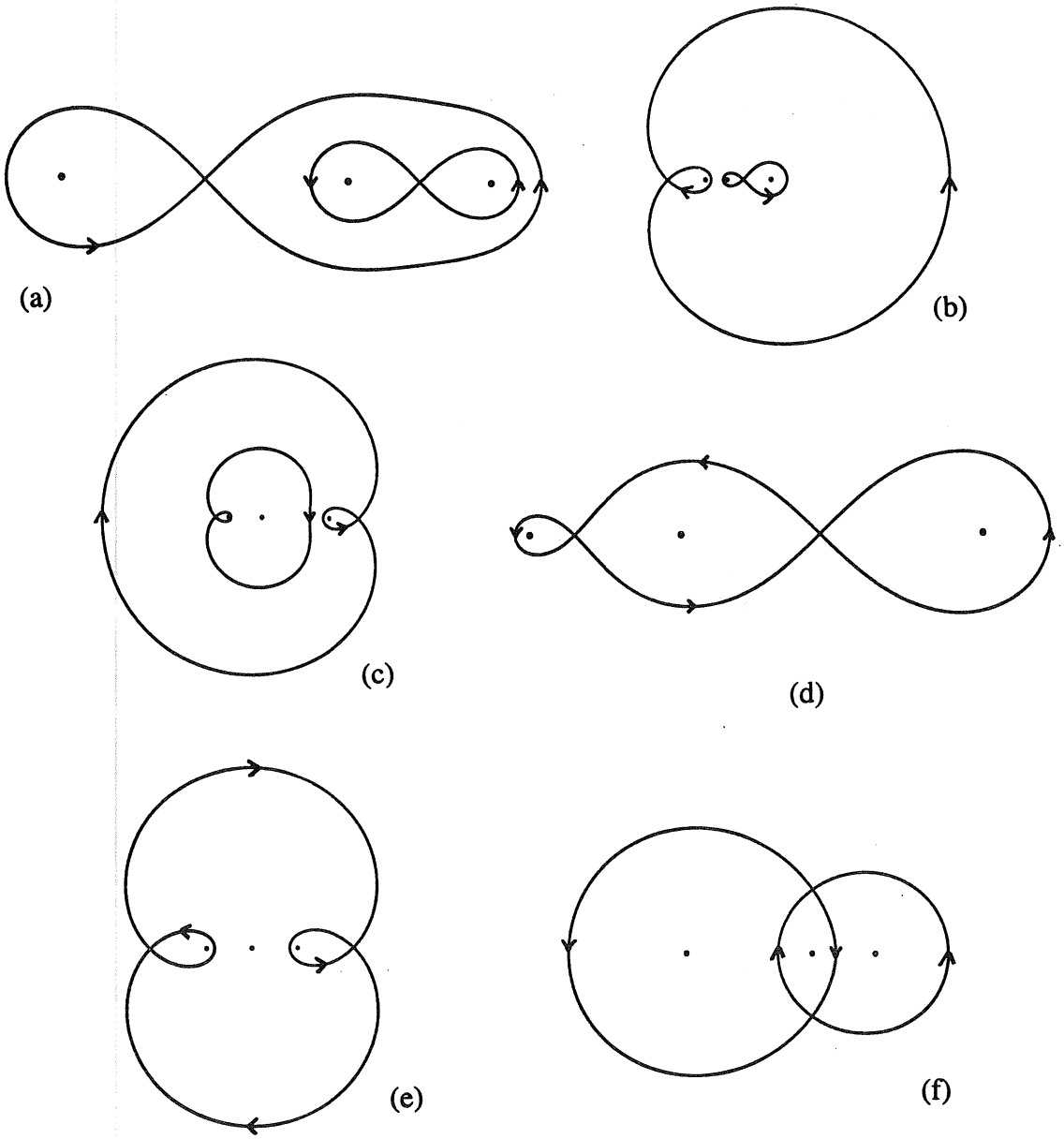

Figure 7: Streamline patterns to scale for certain combinations of vortex strengths and positions. In each case vortices are placed on the x-axis. We list the ratio of vortex strengths from left to right, $\Gamma_1:\Gamma_2:\Gamma_3$, the coordinates (x_1,x_2,x_3), and the comparison panel in Fig.4: (a) 5:3:4, (–2,0,1), cf. Fig.4(a); (b) (–1):1:1, (–1,0,2), cf. Fig.4(c); (c) 1:(–4):1, (–1,0,2), cf. Fig.4(f); (d) 1.863785...:2:3, (–1,0,2), cf. Fig.4(g); (e) 2.244066...:(–4):1, (–1,0,2), cf. Fig.4(j); (f) 5:(–3):4, (–2,0,2), cf. Fig.4(l).

First, for the case of identical vortices, consider the symmetrical configurations in which the vortices form an isosceles triangle. Assume the vortices numbered such that vortex 3 is situated on the perpendicular bisector of the side 12. Then, if vortex 3 is far from 12, the streamline topology must clearly be of the type shown in Fig.4(a) with both stagnation points on the perpendicular bisector of 12 itself (by symmetry). On the other hand, if vortex 3 is on or close to the line 12, the streamline topology must be that of Fig.4(g), with the stagnation points located symmetrically on either side of the

perpendicular bisector of 12. It is clear that for such configurations the streamfunction assumes the same value at both stagnation points. Thus, considering the family of isosceles triangles that arise as vortex 3 is moved along the bisector of 12, we see that there is exactly one point at which the streamline pattern changes from the topology in Fig.4(a) to that of Fig.4(g). At this cross-over point the streamline topology is that of Fig.5(a), which occurs precisely when the vortices form an equilateral triangle.

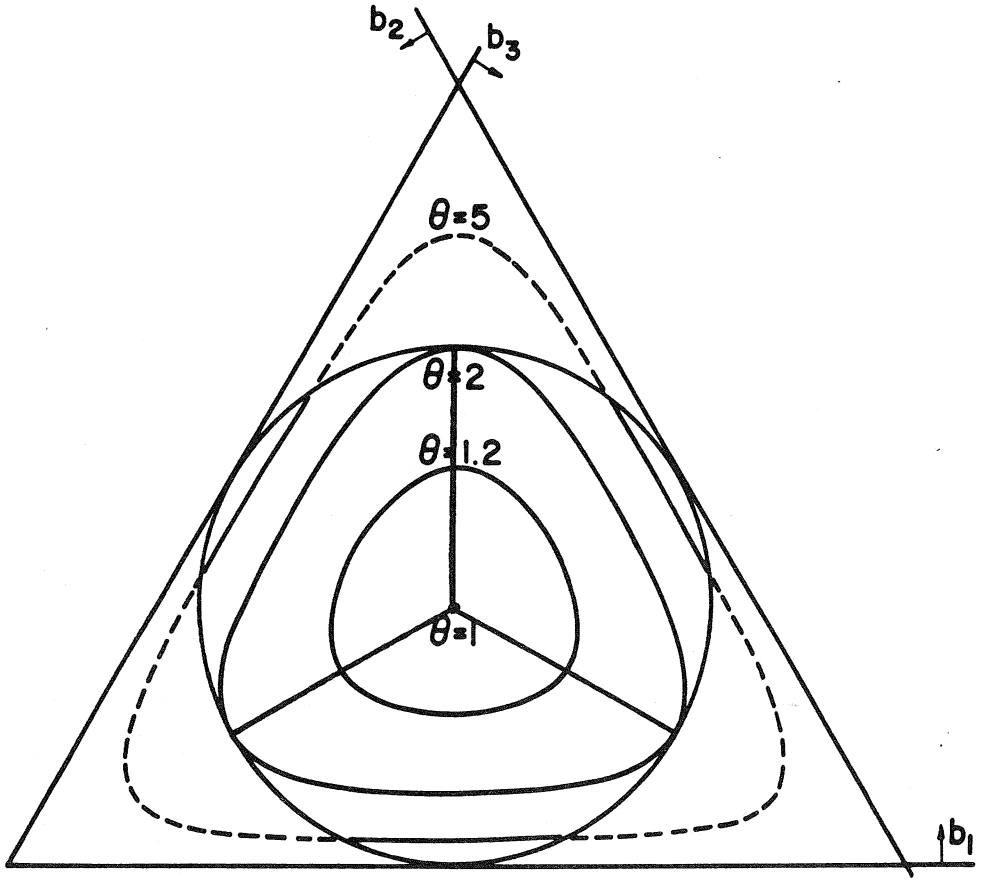

Figure 8: "Phase diagram" for three identical vortices (cf. Aref, 1979) with the three bifurcation lines shown.

Now, let us connect these purely kinematical results to the dynamic problem of the motion of three identical vortices. In Fig.8 we have reproduced the "phase diagram" from Aref (1979; Fig.2) which summarizes the relative motion of the three vortices. The distance of a point in this diagram from the three sides of the equilateral triangle represents the square of the corresponding side in the vortex triangle in the plane of motion. As the vortices move, this "phase point" negotiates one of the curves in the diagram shaped as a "rounded triangle". Because of the triangle inequality, the only physically accessible region of the diagram in Fig.8 is the interior of the circle shown (see Aref, 1979, for additional details). The three line segments radiating out from the centroid of the triangle in Fig.8 correspond to configurations for which the streamline topology is of the type shown in Fig.4(g) (the two equal sides in the isosceles triangle of vortices are shorter than the third side). As the vortices move about, the "phase point" in Fig. 8 will either intersect all three of these radial lines (when $1<\theta<2$ in the notation of Aref, 1979), or will not intersect them

at all (when $\theta>2$). In the former case, the streamline topology is generally that of Fig.4(a), but three times per period it bifurcates, changing for an instant to that of Fig.4(g) as the vortices form an obtuse-angled, isosceles triangle, and then returning to the pattern Fig.4(a) but with two different vortices in the "figure eight" streamline loop. In the second case, the streamline topology is always that of Fig.4(a), and the vortices surrounded by the "figure eight" streamline pattern are always the same two vortices.

It is interesting to note that the orientation of the vortex triangle is invariant in the former case (i.e., when the streamline topology undergoes repeated bifurcations), but switches every time the vortices become collinear in the latter case (although the streamline topology remains the same). In the special case $\theta=1$ the vortices rotate rigidly as an equilateral triangle and the streamline topology is that of Fig.5(a). For $\theta=2$ the vortices are either collinear and uniformly spaced, rotating as a rigid body, in which case the streamline topology is that of Fig.4(g), or they will asymptotically approach such a state, and during the approach the streamline topology will be that of Fig.4(a).

For the case of three identical vortices the inscribed ellipse with foci at the stagnation points of the flow is known as the *Steiner ellipse,* and may be approached in a more elementary way than through the general theory set out in §4. We refer the reader to Schoenberg's (1982) book (in particular Ch.7 §4). Schoenberg quotes and proves an 1888 theorem by van den Berg (which is a special case of Siebeck's theorem).

The case of three vortices with circulations $\Gamma_1 = \Gamma_2 = -\Gamma_3$ proceeds similarly. We are in the hyperbolic case, and so *a priori* we expect to have several possibilities for the instantaneous streamline pattern, viz the cases labelled b, c, d, h, i and l in Fig.4. However, simple inspection shows that of these only c and l are possible. The reason is that in all the other patterns one can find a loop encircling a positive vortex and the negative vortex such that the circulation integral around it is apparently non-zero. This is, of course, impossible since the negative vortex exactly cancels either of the positive vortices. Now we proceed as above. Consider configurations with all three vortices on a line. If vortex 3, the negative vortex, is far away from vortices 1 and 2, the streamline pattern clearly must be of the type in Fig.4(c) with both stagnation points on the line through the vortices. If vortex 3 is situated somewhere between vortices 1 and 2, we find a streamline pattern with the topology of Fig.4(l), and the stagnation points will be symmetrically positioned above and below the line through the vortices. We shall not elaborate the correspondence with the regimes of motion established in the earlier analysis of this problem (Aref, 1979, Fig.4).

6. The 'atmosphere' of a translating vortex system

A related problem, in which the role of stagnation points is also important, is the size and shape of the "atmosphere" of a translating vortex system, i.e., the fluid region carried along by a translating vortex pair, first discussed by Thomson (1867). In this problem we are concerned with the number and location of stagnation points in a frame of reference following the vortices, which are in steady translation. We briefly show how the methodology of the preceding sections can be applied to this problem.

If V is the (complex) velocity of translation, we have for the vortex positions the system of equations

$$\frac{1}{2\pi i}\sum_{\beta=1}^{N}{}' \frac{\Gamma_\beta}{z_\alpha - z_\beta} = V^*, \qquad (6.1)$$

and we wish to solve for the stagnation points in a frame following the vortices, i.e., find the z for which

$$V^* = \frac{1}{2\pi i} \sum_{\alpha=1}^{N} \frac{\Gamma_\alpha}{z - z_\alpha}. \tag{6.2}$$

The situation we are considering implies that the sum of the vortex strengths vanishes, as is easily seen from (6.1) by multiplying it by Γ_α and summing on α.

From (6.1) we find, furthermore, that

$$2\pi i\, V^* (Q + iP) = \sum_{\alpha,\beta=1}^{N\prime} \frac{\Gamma_\alpha \Gamma_\beta z_\alpha}{z_\alpha - z_\beta} = \tfrac{1}{2} \sum_{\alpha,\beta=1}^{N\prime} \Gamma_\alpha \Gamma_\beta, \tag{6.3}$$

where Q and P are the (real) components of the linear impulse:

$$Q + iP = \sum_{\alpha=1}^{N} \Gamma_\alpha z_\alpha. \tag{6.4}$$

Since the vortex strengths sum to zero, we may re-write the right hand side of (6.3) as $-\frac{1}{2}\sum_{\alpha=1}^{N} \Gamma_\alpha^2$.

Thus, recalling the developments in §3, we are led to consider the curve of class N given by the equation

$$\Psi[\mathbf{u}] = (\tfrac{1}{2}\sum_{\alpha=1}^{N} \Gamma_\alpha^2)\, L_1[\mathbf{u}]L_2[\mathbf{u}] \ldots L_N[\mathbf{u}] + (Qu_1 + Pu_2)\, \Phi[\mathbf{u}] = 0. \tag{6.5}$$

According to (6.2), (6.3) and §3 the focal points of this curve, i.e., the solutions of $\Psi[1,i,-z] = 0$, are the stagnation points that we seek.

It is clear that all the lines connecting vortices pairwise are tangents to the curve: $\Psi[\mathbf{u}_{\alpha\beta}] = 0$ by the same argument that we used for the vanishing of $\Phi[\mathbf{u}_{\alpha\beta}]$. It is also clear that the derivatives $\partial\Psi[\mathbf{u}_{\alpha\beta}]/\partial u_i$, i=1,2,3, equal $(Qu_1 + Pu_2)\, \partial\Phi/\partial u_i$ evaluated for $[\mathbf{u}]=[\mathbf{u}_{\alpha\beta}]$. Hence, the points of tangency are, once again, the points $z_{\alpha\beta}^{(S)}$ from (3.29).

Considering the coefficient of the term of order N–1 in the stagnation point (or focal point) equation $\Psi[1,i,-z] = 0$, we see that since the sum of the strengths vanishes, we have the analog of (2.9) that

$$\sum_{n=1}^{N} \left(z_n^{(S)} - z_m\right) = 0, \tag{6.6}$$

where the stagnation points and the midpoint are defined as before but now refer to the situation of a uniformly translating vortex configuration, and the condition of zero velocity in that frame of reference.

a. Two vortices

Consider vortices 1 and 2 with strengths $\Gamma_1 = -\Gamma_2 = \Gamma$, positions $x_1 = x_2 = 0$, $y_1 = -y_2 = Y$. Thus, $Q = 0$ and $P = 2\Gamma Y$. An easy calculation gives

$$\Psi[\mathbf{u}] = \Gamma^2\left(u_3^2 + 3Y^2u_2^2\right). \tag{6.7}$$

This is a singular (line) conic, consisting of two bundles of lines. In one bundle are all lines of the form [u,v,$-i\sqrt{3}$Yv]; in the second all lines of the form [u,v,$i\sqrt{3}$Yv]. Another way of characterizing these line bundles is to note that all the lines in the former bundle pass through the point C_+ with coordinates (0, $i\sqrt{3}$Y,1); all the lines in the second pass through C_- with coordinates (0, $-i\sqrt{3}$Y,1).

To find the 'foci' of this singular conic we ask which lines in either bundle pass through the circular points at infinity (see §3(d)). The coordinates of the four lines $IC_\pm$ and $JC_\pm$ are:

$$\begin{aligned} &IC_+ : [i,-1,i\sqrt{3}Y] \quad ; \quad JC_+ : [-i,-1,i\sqrt{3}Y] \\ &IC_- : [i,-1,-i\sqrt{3}Y] \quad ; \quad JC_- : [-i,-1,-i\sqrt{3}Y] \end{aligned} \tag{6.8}$$

The two finite points of intersection of these four lines are the affine points ($\pm\sqrt{3}$Y,0), i.e., precisely the forward and rear stagnation points of the vortex pair "atmosphere." The vortices and either stagnation point form an equilateral triangle.

b. Three vortices

We again adopt triangular coordinates, X_1, X_2, X_3, based on the triangle spanned by the vortices and the conjugate linear coordinates U_1, U_2, U_3, as in §4. We then have $L_i[\mathbf{u}] = -U_i$, i=1,2,3. Also, since $\xi_i u_1 + \eta_i u_2 + u_3 = U_i$, i=1,2,3, we see that

$$Qu_1 + Pu_2 = \Gamma_1U_1 + \Gamma_2U_2 + \Gamma_3U_3. \tag{6.9}$$

Thus, $\Psi[\mathbf{U}] = 0$ becomes

$$\begin{aligned} &(\Gamma_1\Gamma_2+\Gamma_2\Gamma_3+\Gamma_3\Gamma_1)U_1U_2U_3 + \\ &\qquad (\Gamma_1U_1+\Gamma_2U_2+\Gamma_3U_3)(\Gamma_1U_2U_3+\Gamma_2U_3U_1+\Gamma_3U_1U_2) = 0. \end{aligned} \tag{6.10}$$

This is the equation of a curve of class 3. It has three distinct, real foci, in general, and these are the stagnation points in the co-moving frame.

From the solution of the three-vortex problem (Aref, 1979; Rott, 1989, Aref 1989) we know that for the translating configurations the three vortices must be at the vertices of an equilateral triangle. Let $\omega = e^{i2\pi/3}$ and let vortex α=1,2,3 be at $z_\alpha = a\,\omega^\alpha$, i.e., vortex 1 is at z_1=aω, vortex 2 at z_2=aω^*, and vortex 3 at z_3=a. We introduce the notation

$$\gamma_n = \Gamma_1 + \Gamma_2\omega^n + \Gamma_3\omega^{*n} \quad ; \quad n = 0,\ 1,\ 2, \tag{6.11}$$

such that γ_0, γ_1, γ_2 are the components of the discrete Fourier transform of Γ_1, Γ_2, Γ_3. Clearly, γ_0=0 and γ_1, γ_2 are complex conjugates; also, $Q + iP = a\omega\gamma_1$.

Note that

$$\gamma_1\gamma_2 = \Gamma_1^2+\Gamma_2^2+\Gamma_3^2-\Gamma_1\Gamma_2-\Gamma_2\Gamma_3-\Gamma_3\Gamma_1 = \tfrac{3}{2}\left(\Gamma_1^2+\Gamma_2^2+\Gamma_3^2\right), \tag{6.12}$$

where the last expression follows from $\gamma_0^2 = \Gamma_1^2+\Gamma_2^2+\Gamma_3^2+2\Gamma_1\Gamma_2+2\Gamma_2\Gamma_3+2\Gamma_3\Gamma_1 = 0$.

The equation determining the stagnation points is

$$\Psi[1,i,-z] = \tfrac{1}{3}\gamma_1\gamma_2\,(z^3-a^3) + a\omega\gamma_1(a\omega\gamma_1 z + a^2\omega^*\gamma_2) = 0, \tag{6.13}$$

or, with $\zeta = z/a$,

$$\zeta^3 + 3(\gamma_1/\gamma_2)\omega^*\,\zeta + 2 = 0. \tag{6.14}$$

Since γ_1 and γ_2 are complex conjugates, the coefficient of ζ is always of modulus 1. In the special case $\Gamma_1=\Gamma_2=-\Gamma_3/2$ the ratio $\gamma_1/\gamma_2 = \omega$ and Eq.(6.14) becomes simply

$$\zeta^3 + 3\zeta + 2 = 0. \tag{6.15}$$

The solutions to (6.14) may be found by elementary methods. It may be worth noting that the three stagnation points are always distinct.[7]

7. Concluding remarks

Determining the number, nature and location of stagnation points for a system of point vortices is, clearly, one of the simplest problems of its kind. The stagnation points in this case are the roots of a certain polynomial, and calculating them for a given configuration of vortices of known strengths is, in principle, elementary. However, a geometrical characterization of the location of stagnation points, and an understanding of how they move when the strengths and/or positions of the vortices are changed, leads to less familiar mathematical problems, and tools such as the algebraic geometry developed by Plücker and Siebeck a century ago and the use of the complex projective plane appear to be useful. The most interesting result that we have obtained is for the case of three vortices of zero net circulation, where a "similarity law" for the location of the single stagnation point emerges.

The approach of this paper does not appear to be particularly useful if the number of vortices is large, since the order of the polynomial giving Siebeck's curve is then unmanageably large, and the best one can do is probably to determine all stagnation points numerically at every step of the motion. For a small number of vortices, on the other hand, the algebraic-geometric specification of stagnation points presented here is as precise as one can hope to achieve.

The location of stagnation points is intimately connected with the topology of the streamline pattern of the flow induced by the vortices. The possible streamline topologies can be found by the process illustrated here for three vortices of assembling such patterns by substituting for a vortex in a pattern for N vortices one of the patterns for two vortices (Fig.3) and thus arriving at a streamline pattern for N+1 vortices. For simple choices of the vortex strengths it was possible to describe transitions between different streamline

7) The vanishing of the discriminant of the cubic (6.14) implies that $(\gamma_1/\gamma_2)^3 = -1$, i.e., $\gamma_1/\gamma_2 = -1, -\omega, -\omega^*$, and each of these three possibilities implies that one of the vortex strengths vanishes.

topologies as the vortices move.

Taken together the results of this paper provide some guidance in determining the stagnation points and streamline topology for a small number of vortices.

Acknowledgements

We are indebted to P. L. Boyland, V. V. Meleshko and M. A. Stremler for comments and discussion on several aspects of this work, including flow topology and the history of vortex motion. Mark Stremler kindly wrote the program used to produce the streamline plots of Fig.7. This work was supported by National Science Foundation grant CTS–9311545.

References

Aref, H. 1979 Motion of three vortices. *Phys. Fluids* **22**, 393-400.

Aref, H. 1989 Three vortex motion with zero total circulation: Addendum *J. Appl. Math. Phys. (ZAMP)* **40**, 495-500.

Aref, H. 1992 Trilinear coordinates in fluid mechanics. In *Studies in Turbulence,* T. B. Gatski, S. Sarker & C. G. Speziale, eds., Springer-Verlag, pp.568-581.

Aref, H. & Brøns, M. 1995 On stagnation points in vortex flows. *Bull. Amer. Phys. Soc.* **40**, 1921.

Coxeter, H. S. M. 1993 *The Real Projective Plane.* Third ed., Springer-Verlag.

Eckhardt, B. 1988 Integrable four-vortex motion. *Phys. Fluids* **31**, 2796-2801.

Eckhardt, B. & Aref, H. 1988 Integrable and chaotic motions of four vortices II: Collision dynamics of vortex pairs. *Phil. Trans. R. Soc. (London) A* **326**, 655-696.

Ferrers, N. M. 1866 *An Elementary Treatise on Tri-linear Coordinates, the Method of Reciprocal Polars and the Theory of Projections.* Second ed., Macmillan & Co.

Heawood, P. J. 1906 Geometrical relations between the roots of $f(x) = 0$ and $f'(x) = 0$. *Q. J. Math.* **38**, 84-107.

Lamb, H. 1932 *Hydrodynamics.* Sixth ed., Cambridge Univ. Press (republ. by Dover Publ., Inc.) §154.

Marden, M. 1949 *Geometry of Polynomials.* Amer. Math. Soc., 243 pp.

Morton, W. B. 1932 On the motion near two straight parallel vortices. *Proc. R. Irish. Acad. A* **41**, 1-7.

Rott, N. 1989 Three vortex motion with zero total circulation. *J. Appl. Math. Phys. (ZAMP)* **40**, 473-494.

Salmon, G. 1854 *A treatise on conic sections.* Sixth ed., Chelsea, New York.

Schoenberg, I. J. 1982 *Mathematical Time Exposures.* The Mathematical Association of America, Inc.

Siebeck, F. H. 1864 Ueber eine neue analytische Behandlungsweise der Brennpunkte. *J. Reine Angew. Math.* **64**, 175-182.

Synge, J. L. 1949 On the motion of three vortices. *Can. J. Math.* **1**, 257-270.

Thomson, W. (Lord Kelvin) 1867 On Vortex Atoms. *Proc. R. Soc. Edinburgh* **6**, 94-105.

List of Recent TAM Reports

No.	Authors	Title	Date
763	Man., C. S., and D. E. Carlson	On the traction problem of dead loading in linear elasticity with initial stress—*Archive for Rational Mechanics and Analysis* **128**, 223–247 (1994)	Aug. 1994
764	Zhang, Y., and R. L. Weaver	Leaky Rayleigh wave scattering from elastic media with random microstructures—*Journal of the Acoustical Society of America* **99**, 88–99 (1996)	Aug. 1994
765	Cortese, T. A., and S. Balachandar	High-performance spectral simulation of turbulent flows in massively parallel machines with distributed memory—*International Journal of Supercomputer Applications* **9**, 185–202 (1995)	Aug. 1994
766	Balachandar, S.	Signature of the transition zone in the tomographic results extracted through the eigenfunctions of the two-point correlation—*Geophysical Research Letters* **22**, 1941–1944 (1995)	Sept. 1994
767	Piomelli, U.	Large-eddy simulation of turbulent flows	Sept. 1994
768	Harris, J. G., D. A. Rebinsky, and G. R. Wickham	An integrated model of scattering from an imperfect interface—*Journal of the Acoustical Society of America* **99**, 1315–1325 (1996)	Sept. 1994
769	Hsia, K. J., and Z.-Q. Xu	The mathematical framework and an approximate solution of surface crack propagation under hydraulic pressure loading—*International Journal of Fracture*, in press (1996)	Sept. 1994
770	Balachandar, S.	Two-point correlation and its eigen-decomposition for optimal characterization of mantle convection	Oct. 1994
771	Lufrano, J. M., and P. Sofronis	Numerical analysis of the interaction of solute hydrogen atoms with the stress field of a crack—*International Journal of Solids and Structures*, **33**, 1709–1723 (1996)	Oct. 1994
772	Aref, H., and S. W. Jones	Motion of a solid body through ideal fluid—Proceedings of the DCAMM 25th Anniversary Volume, 55–68 (1994)	Oct. 1994
773	Stewart, D. S., T. D. Aslam, J. Yao, and J. B. Bdzil	Level-set techniques applied to unsteady detonation propagation—In "Modeling in Combustion Science," *Lecture Notes in Physics* , eds. J. Buckmaster and J. Takeno **126**, 390–409 (1996)	Oct. 1994
774	Mittal, R., and S. Balachandar	Effect of three-dimensionality on the lift and drag of circular and elliptic cylinders—*Physics of Fluids* **7**, 1841–1865 (1995)	Oct. 1994
775	Stewart, D. S., T. D. Aslam, and J. Yao	On the evolution of cellular detonation	Nov. 1994 *Revised* Jan. 1996
776	Aref, H.	On the equilibrium and stability of a row of point vortices—*Journal of Fluid Mechanics* **290**, 167–181 (1995)	Nov. 1994
777	Cherukuri, H. P., T. G. Shawki, and M. El-Raheb	An accurate finite-difference scheme for elastic wave propagation in a circular disk—*Journal of the Acoustical Society of America*, in press (1996)	Nov. 1994
778	Li, L., and N. R. Sottos	Improving hydrostatic performance of 1–3 piezocomposites—*Journal of Applied Physics* **77**, 4595–4603 (1995)	Dec. 1994
779	Phillips, J. W., D. L. de Camara, M. D. Lockwood, and W. C. C. Grebner	Strength of silicone breast implants—*Plastic and Reconstructive Surgery* **97**, 1215–1225 (1996)	Jan. 1995
780	Xin, Y.-B., K. J. Hsia, and D. A. Lange	Quantitative characterization of the fracture surface of silicon single crystals by confocal microscopy—*Journal of the American Ceramics Society* **78**, 3201–3208 (1995)	Jan. 1995
781	Yao, J., and D. S. Stewart	On the dynamics of multi-dimensional detonation—*Journal of Fluid Mechanics* **309**, 225–275 (1996)	Jan. 1995
782	Riahi, D. N., and T. L. Sayre	Effect of rotation on the structure of a convecting mushy layer—*Acta Mechanica* **118**, 109–120 (1996)	Feb. 1995
783	Batchelor, G. K., and TAM faculty and students	A conversation with Professor George K. Batchelor	Feb. 1995

List of Recent TAM Reports (cont'd)

No.	Authors	Title	Date
784	Sayre, T. L., and D. N. Riahi	Effect of rotation on flow instabilities during solidification of a binary alloy—*International Journal of Engineering Science* **34**, 1631–1645 (1996)	Feb. 1995
785	Xin, Y.-B., and K. J. Hsia	A technique to generate straight surface cracks for studying the dislocation nucleation condition in brittle materials—*Acta Metallurgica et Materialia* **44**, 845–853 (1996)	Mar. 1995
786	Riahi, D. N.	Finite bandwidth, long wavelength convection with boundary imperfections: Near-resonant wavelength excitation—*International Journal of Mathematics and Mathematical Sciences*, in press (1996)	Mar. 1995
787	Turner, J. A., and R. L. Weaver	Average response of an infinite plate on a random foundation—*Journal of the Acoustical Society of America* **99**, 2167–2175 (1996)	Mar. 1995
788	Weaver, R. L., and D. Sornette	The range of spectral correlations in pseudointegrable systems: GOE statistics in a rectangular membrane with a point scatterer—*Physical Review E* **52**, 341 (1995)	Apr. 1995
789	Students in TAM 293–294	Thirty-second student symposium on engineering mechanics, J. W. Phillips, coordinator: Selected senior projects by K. F. Anderson, M. B. Bishop, B. C. Case, S. R. McFarlin, J. M. Nowakowski, D. W. Peterson, C. V. Robertson, and C. E. Tsoukatos	Apr. 1995
790	Figa, J., and C. J. Lawrence	Linear stability analysis of a gravity-driven Newtonian coating flow on a planar incline	May 1995
791	Figa, J., and C. J. Lawrence	Linear stability analysis of a gravity-driven viscosity-stratified Newtonian coating flow on a planar incline	May 1995
792	Cherukuri, H. P., and T. G. Shawki	On shear band nucleation and the finite propagation speed of thermal disturbances—*International Journal of Solids and Structures*, in press (1996)	May 1995
793	Harris, J. G.	Modeling scanned acoustic imaging of defects at solid interfaces—Chapter in *IMA Workshop on Inverse Problems in Wave Propagation*, eds. G. Chevant, G. Papanicolaou, P. Sacks and W. E. Symes, 237–258, Springer-Verlag, New York (1996)	May 1995
794	Sottos, N. R., J. M. Ockers, and M. J. Swindeman	Thermoelastic properties of plain weave composites for multilayer circuit board applications	May 1995
795	Aref, H., and M. A. Stremler	On the motion of three point vortices in a periodic strip—*Journal of Fluid Mechanics* **314**, 1–25 (1996)	June 1995
796	Barenblatt, G. I., and N. Goldenfeld	Does fully-developed turbulence exist? Reynolds number independence versus asymptotic covariance—*Physics of Fluids* **7**, 3078–3082 (1995)	June 1995
797	Aslam, T. D., J. B. Bdzil, and D. S. Stewart	Level set methods applied to modeling detonation shock dynamics—*Journal of Computational Physics*, **126**, 390–409 (1996)	June 1995
798	Nimmagadda, P. B. R., and P. Sofronis	The effect of interface slip and diffusion on the creep strength of fiber and particulate composite materials—Proceedings of the ASME Applied Mechanics Division **213**, 125–143 (1995)	July 1995
799	Hsia, K. J., T.-L. Zhang, and D. F. Socie	Effect of crack surface morphology on the fracture behavior under mixed mode loading—*ASTM Special Technical Publication* 1296, in press (1996)	July 1995
800	Adrian, R. J.	Stochastic estimation of the structure of turbulent fields—*Eddy Structure Identification*, ed. J. P. Bonnet, Springer: Berlin 145–196 (1996)	Aug. 1995
801	Riahi, D. N.	Perturbation analysis and modeling for stratified turbulence	Aug. 1995
802	Thoroddsen, S. T.	Conditional sampling of dissipation in high Reynolds number turbulence—*Physics of Fluids* **8**, 1333–1335	Aug. 1995
803	Riahi, D. N.	On the structure of an unsteady convecting mushy layer—*Acta Mechanica*, in press (1996)	Aug. 1995

List of Recent TAM Reports (cont'd)

No.	Authors	Title	Date
804	Meleshko, V. V.	Equilibrium of an elastic rectangle: The Mathieu–Inglis–Pickett solution revisited—*Journal of Elasticity* **40**, 207–238 (1995)	Aug. 1995
805	Jonnalagadda, K., G. E. Kline, and N. R. Sottos	Local displacements and load transfer in shape memory alloy composites	Aug. 1995
806	Nimmagadda, P. B. R., and P. Sofronis	On the calculation of the matrix–reinforcement interface diffusion coefficient in composite materials at high temperatures—*Acta Metallurgica et Materialia*, **44**, 2711–2716 (1996)	Aug. 1995
807	Carlson, D. E., and D. A. Tortorelli	On hyperelasticity with internal constraints—*Journal of Elasticity* **42**, 91–98 (1966)	Aug. 1995
808	Sayre, T. L., and D. N. Riahi	Oscillatory instabilities of the liquid and mushy layers during solidification of alloys under rotational constraint—*Acta Mechanica*, in press (1996)	Sept. 1995
809	Xin, Y.-B., and K. J. Hsia	Simulation of the brittle–ductile transition in silicon single crystals using dislocation mechanics	Oct. 1995
810	Ulysse, P., and R. E. Johnson	A plane-strain upper-bound analysis of unsymmetrical single-hole and multi-hole extrusion processes	Oct. 1995
811	Fried, E.	Continua described by a microstructural field—*Zeitschrift für angewandte Mathematik und Physik*, **47**, 168–175 (1996)	Nov. 1995
812	Mittal, R., and S. Balachandar	Autogeneration of three-dimensional vortical structures in the near wake of a circular cylinder	Nov. 1995
813	Segev, R., E. Fried, and G. de Botton	Force theory for multiphase bodies—*Journal of Geometry and Physics*, in press (1996)	Dec. 1995
814	Weaver, R. L.	The effect of an undamped finite-degree-of-freedom "fuzzy" substructure: Numerical solutions and theoretical discussion—*Journal of the Acoustical Society of America* **100**, 3159–3164 (1996)	Jan. 1996
815	Haber, R. B., C. S. Jog, and M. P. Bendsøe	A new approach to variable-topology shape design using a constraint on perimeter—*Structural Optimization* **11**, 1–12 (1996)	Feb. 1996
816	Xu, Z.-Q., and K. J. Hsia	A numerical solution of a surface crack under cyclic hydraulic pressure loading	Mar. 1996
817	Adrian, R. J.	Bibliography of particle velocimetry using imaging methods: 1917–1995—*Produced and distributed in cooperation with TSI, Inc., St. Paul, Minn.*	Mar. 1996
818	Fried, E., and G. Grach	An order-parameter based theory as a regularization of a sharp-interface theory for solid–solid phase transitions—*Archive for Rational Mechanics and Analysis*, in press (1996)	Mar. 1996
819	Vonderwell, M. P., and D. N. Riahi	Resonant instability mode triads in the compressible boundary-layer flow over a swept wing—*Physics of Fluids*, in press (1996)	Mar. 1996
820	Short, M., and D. S. Stewart	Low-frequency two-dimensional linear instability of plane detonation—*Journal of Fluid Mechanics*, in press (1997)	Mar. 1996
821	Casagranda, A., and P. Sofronis	On the scaling laws for the consolidation of nanocrystalline powder compacts—Proceedings of the IUTAM Symposium on the Mechanics of Granular and Porous Materials (1996)	Apr. 1996
822	Xu, S., and D. S. Stewart	Deflagration-to-detonation transition in porous energetic materials: A comparative model study—*Journal of Fluid Mechanics*, in press (1997)	Apr. 1996
823	Weaver, R. L.	Mean and mean-square responses of a prototypical master/fuzzy structure—*Journal of the Acoustical Society of America*, in press (1996)	Apr. 1996
824	Fried, E.	Correspondence between a phase-field theory and a sharp-interface theory for crystal growth—*Continuum Mechanics and Thermodynamics*, in press (1997)	Apr. 1996
825	Students in TAM 293–294	Thirty-third student symposium on engineering mechanics, J. W. Phillips, coordinator: Selected senior projects by W. J. Fortino II, A. A. Mordock, and M. R. Sawicki	May 1995

List of Recent TAM Reports (cont'd)

No.	Authors	Title	Date
826	Riahi, D. N.	Effects of roughness on nonlinear stationary vortices in rotating disk flows—*Mathematical and Computer Modeling*, in press (1996)	June 1996
827	Riahi, D. N.	Nonlinear instabilities of shear flows over rough walls	June 1996
828	Weaver, R. L.	Multiple scattering theory for a plate with sprung masses: Mean and mean-square responses	July 1996
829	Moser, R. D., M. M. Rogers, and D. W. Ewing	Self-similarity of time-evolving plane wakes	July 1996
830	Lufrano, J. M., and P. Sofronis	Enhanced hydrogen concentrations ahead of rounded notches and cracks—Competition between plastic strain and hydrostatic constraint	July 1996
831	Riahi, D. N.	Effects of surface corrugation on primary instability modes in wall-bounded shear flows	Aug. 1996
832	Bechel, V. T., and N. R. Sottos	Measuring debond length in the fiber pushout test—Proceedings of the ASME Mechanics and Materials Conference (1996)	Aug. 1996
833	Riahi, D. N.	Effect of centrifugal and Coriolis forces on chimney convection during alloy solidification—*Journal of Crystal Growth*, in press (1997)	Sept. 1996
834	Cermelli, P., and E. Fried	The influence of inertia on configurational forces in a deformable solid—*Proceedings of the Royal Society of London A*, in press (1996)	Oct. 1996
835	Riahi, D. N.	On the stability of shear flows with combined temporal and spatial imperfections	Oct. 1996
836	Carranza, F. L., B. Fang, and R. B. Haber	An adaptive space–time finite element model for oxidation-driven fracture	Nov. 1996
837	Carranza, F. L., B. Fang, and R. B. Haber	A moving cohesive interface model for fracture in creeping materials	Nov. 1996
838	Balachandar, S., R. Mittal, and F. M. Najjar	Properties of the mean wake recirculation region in two-dimensional bluff body wakes	Dec. 1996
839	Ti, B. W., W. D. O'Brien, Jr., and J. G. Harris	Measurements of coupled Rayleigh wave propagation in an elastic plate	Dec. 1996
840	Phillips, W. R. C.	On finite-amplitude rotational waves in viscous shear flows	Jan. 1997
841	Riahi, D. N.	Direct resonance analysis and modeling for a turbulent boundary layer over a corrugated surface	Jan. 1997
842	Liu, Z. C., R. J. Adrian, C. D. Meinhart, and W. Lai	Structure of a turbulent boundary layer using a stereoscopic, large format video-PIV	Jan. 1997
843	Fang, B., F. L. Carranza, and R. B. Haber	An adaptive discontinuous Galerkin methods for viscoplastic analysis	Jan. 1997
844	Xu, S., T. D. Aslam, and D. S. Stewart	High-resolution numerical simulation of ideal and non-ideal compressible reacting flows with embedded internal boundaries	Jan. 1997
845	Zhou, J., C. D. Meinhart, S. Balachandar, and R. J. Adrian	Formation of coherent hairpin packets in wall turbulence	Feb. 1997
846	Lufrano, J. M., P. Sofronis, and H. K. Birnbaum	Elastoplastically accommodated hydride formation and embrittlement	Feb. 1997
847	Keane, R. D., N. Fujisawa, and R. J. Adrian	Unsteady non-penetrative thermal convection from non-uniform surfaces	Feb. 1997
848	Aref, H., and M. Brøns	On stagnation points and streamline topology in vortex flows	Mar. 1997